



Lawrence Berkeley Laboratory

UNIVERSITY OF CALIFORNIA

RECEIVED
LAWRENCE
BERKELEY LABORATORY

AUG 27 1984

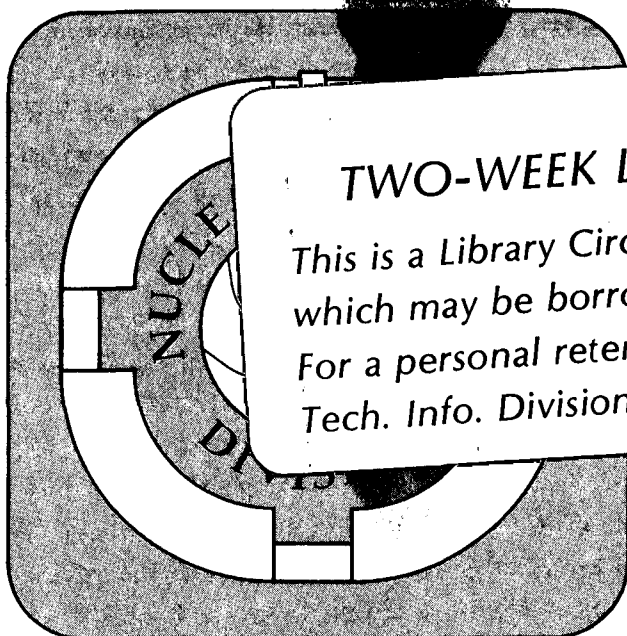
LIBRARY AND
DOCUMENTS SECTION

Submitted to Nuclear Physics A

PARTICLE-GAMMA COINCIDENCE MEASUREMENTS IN
 $^{12}\text{C} + ^{12}\text{C}$ AND $^{12}\text{C} + \text{Pb}$ COLLISIONS AT
2.1 GeV/NUCLEON INCIDENT ENERGY

G. Roche, J. Carroll, C.C. Chang, T. Hallman,
P.N. Kirk, R. Koontz, G. Krebs, L. Madansky,
T. Mulera, H.G. Pugh, L.S. Schroeder, and
J. Vicente

July 1984



TWO-WEEK LOAN COPY

This is a Library Circulating Copy
which may be borrowed for two weeks.
For a personal retention copy, call
Tech. Info. Division, Ext. 6782.

DISCLAIMER

This document was prepared as an account of work sponsored by the United States Government. While this document is believed to contain correct information, neither the United States Government nor any agency thereof, nor the Regents of the University of California, nor any of their employees, makes any warranty, express or implied, or assumes any legal responsibility for the accuracy, completeness, or usefulness of any information, apparatus, product, or process disclosed, or represents that its use would not infringe privately owned rights. Reference herein to any specific commercial product, process, or service by its trade name, trademark, manufacturer, or otherwise, does not necessarily constitute or imply its endorsement, recommendation, or favoring by the United States Government or any agency thereof, or the Regents of the University of California. The views and opinions of authors expressed herein do not necessarily state or reflect those of the United States Government or any agency thereof or the Regents of the University of California.

PARTICLE-GAMMA COINCIDENCE
MEASUREMENTS IN $^{12}\text{C} + ^{12}\text{C}$ and $^{12}\text{C} + \text{Pb}$
COLLISIONS AT 2.1 GeV/NUCLEON INCIDENT ENERGY

G. ROCHE^{a)}, J. CARROLL^{c)}, C.C. CHANG^{d)}, T. HALLMAN^{b)},
P.N. KIRK^{e)}, R. KOONTZ^{a)}, G. KREBS^{e)}, L. MADANSKY^{b)},
T. MULERA^{a)}, H. G. PUGH^{a)}, L. S. SCHROEDER^{a)}, J. VICENTE^{f)}

- a) Lawrence Berkeley Laboratory, University of California, Berkeley, California 94720
- b) The Johns Hopkins University, Baltimore, Maryland 21218
- c) University of California, Los Angeles, California 90024
- d) University of Maryland, College Park, Maryland 20742
- e) Louisiana State University, Baton Rouge, Louisiana 70803
- f) Universite de Clermont II-IN2P3, 63170 Aubiere, France

This work was supported by the Director, Office of Energy Research, Division of Nuclear Physics of the Office of High Energy and Nuclear Physics of the U.S. Department of Energy under Contracts DE-AC03-76SF00098, DE-AS05-76ER04699, DE-AC02-76ER03274 and DE-AT03-81ER40027.

PARTICLE-GAMMA COINCIDENCE
MEASUREMENTS IN $^{12}\text{C} + ^{12}\text{C}$ and $^{12}\text{C} + \text{Pb}$
COLLISIONS AT 2.1 GeV/NUCLEON INCIDENT ENERGY

G. ROCHE^{a)}, J. CARROLL^{c)}, C.C. CHANG^{d)}, T. HALLMAN^{b)},
P.N. KIRK^{e)}, R. KOONTZ^{a)}, G. KREBS^{e)}, L. MADANSKY^{b)},
T. MULERA^{a)}, H. G. PUGH^{a)}, L. S. SCHROEDER^{a)}, J. VICENTE^{f)}

- a) Lawrence Berkeley Laboratory, University of California, Berkeley,
California 94720
- b) The Johns Hopkins University, Baltimore, Maryland 21218
- c) University of California, Los Angeles, California 90024
- d) University of Maryland, College Park, Maryland 20742
- e) Louisiana State University, Baton Rouge, Louisiana 70803
- f) Universite de Clermont II-IN2P3, 63170 Aubiere, France

ABSTRACT

A particle-gamma coincidence experiment has been performed with a 2.1 GeV per nucleon ^{12}C beam from the Bevalac. Data were taken with C and Pb targets. The γ -ray spectra are almost independent of the energy or the kind of charged particles detected in coincidence, mainly protons and deuterons. These γ -ray spectra are interpreted as resulting from π^0 decay, and are consistent with known π^0 production rates. A search for a possible decay of singly charged anomalons into a gamma and a deuteron (or unbound proton-neutron system) has been done by studying the γ -p and γ -d invariant mass distributions. The upper limits for such a process are found to be 2 to 20% of the deuteron production rate, for anomalon masses from 200 to 400 MeV above the deuteron mass, with an anomalon mean lifetime of up to 10^{-9} s, depending on which kind of decay process is considered.

I. INTRODUCTION

High-energy γ -rays observed in relativistic heavy ion collisions at incident energies in the range 1-2 GeV per nucleon are mainly produced through π^0 decay. Other possible weak contributions are nucleus-nucleus bremsstrahlung, η -meson and radiative $\Delta(1232)$ decays. Up to now, only a few experimental studies have been done on this subject. DeJarnette et al.⁽¹⁾ and Hallman⁽²⁾ were mainly interested in the production rate of π^0 's as a function of beam energy in central collisions of ^{12}C and ^{40}Ar on ^{208}Pb . Budiansky⁽³⁾ and Budiansky et al.⁽⁴⁾ have measured single high-energy γ -ray spectra and provided information on the production of bremsstrahlung photons and of π^0 's, η 's and Δ 's in nucleus-nucleus collisions at these energies.

More recently, γ -ray measurements have been performed to study projectile fragments having an anomalously short interaction length, i.e., the so-called anomalous. Evidence for anomalous lengths was first obtained in cosmic-ray exposures^(5,6) and is now supported by emulsion results from accelerator experiments^(7,8) and by reanalysis of old cosmic-ray data⁽⁹⁾ although recent results⁽¹⁰⁻¹⁵⁾ are controversial. Besides the fact that anomalous (if they exist) have a much shorter interaction length and are stable against strong interaction decay, nothing else is presently known and it is evidently desirable to identify additional features. Liss et al.⁽¹⁵⁾ have searched for single delayed gammas as a possible decay process. Their negative result does not completely rule out a possible electromagnetic decay of an anomalous state, because their measurement was done at 940 MeV per nucleon, an energy at which it has been suggested⁽⁸⁾ that the effect may not be produced.

We have taken a different approach to the study of anomalous fragments. First, the study is done in the target fragmentation region; second, we look for singly charged anomalous fragments through particle-gamma coincidence measurements. The first point does not need much comment; if anomalous exist in the projectile fragmentation region as indicated by nuclear emulsion experiments, they should also be produced in the target region in which they are better detected by the experimental method we are using. Secondly, we have focused on the creation and detection of singly charged fragments which have been studied by Judek⁽⁶⁾. For interactions with primary energies up to

5 GeV per nucleon, fragments are found to be anomalous in the range of transverse momenta 120–480 MeV/c, which corresponds in the target region to deuterons of energies in the range 4–60 MeV. On the theoretical side, Frederiksson et al.⁽¹⁶⁾ suggest the existence of a possible six-quark deuteron state that we estimate could produce a γ -ray around 200–300 MeV. Our experimental method consists then in looking for any sharp line or bump⁽¹⁷⁾ in the γ -ray spectra in coincidence with deuterons and protons and, ultimately, looking for any signal in the particle-gamma invariant mass distributions. Besides this specific aim, our measurements will bring complementary information on the physics first mentioned in the paper. This is the first particle-gamma coincidence experiment performed at Bevalac energies.

The remaining plan of this paper is as follows : Section II describes the experimental setup along with test run results; Section III gives the γ -ray spectra and their analysis in terms of the number of π^0 's per trigger and the associated π^0 inverse exponential slope; Section IV presents the invariant mass distributions, limits of cross sections for producing anomalous and the possible lifetime effect on our measurements. Conclusions are summarized in Section V.

II. EXPERIMENTAL SETUP AND TEST RESULTS

The experiment was performed with a 2.1 GeV per nucleon ^{12}C beam from the Bevalac at the Lawrence Berkeley Laboratory. Data were taken with C and Pb targets.

The experimental configuration is shown in Fig. 1. The multiwire proportional chambers WC2 and WC3 were used for beam alignment and the ionization chamber IC for beam intensity measurement. Photons and charged particles produced in the target T were detected in a thick NaI crystal system (NAI) and two ΔE -E telescopes (TEL2, TEL3), respectively. The γ -ray detector system NAI consists of a plastic scintillator V used as a charged particle veto, a 2.54-cm thick NaI crystal in which the shower is generated, a plastic scintillator C which detects the γ -ray conversion, and two 12.7-cm thick NaI crystals in which the shower deposits the rest of its energy. The annular plastic scintillator H signal was also used off-line as a veto to better select the showers emitted around the central axis of the system. The diameters are 25.4 cm for the NaI crystals and 12.7 cm for the conversion detector C. The neutron contamination is estimated to be less than $\sim 1\%$, and the overall resolution was determined to be $\sim 30\%$ at 130 MeV (for minimum ionizing cosmic ray muons). The telescope TEL2 consists of two 1-mm thick silicon detectors with a 7.62-cm NaI crystal, and TEL3 consists of five identical elements made with a plastic scintillator (1.27-cm) and a 12.7-cm NaI crystal. The overall resolutions for TEL2 and TEL3 are, respectively, ~ 10 MeV at 50 MeV and 7 MeV at 100 MeV, for protons. The angles between the beam direction and the detector axes are 41° for TEL2, 45° for TEL3, and 124° for NAI, and the azimuthal angles between TEL2 and NAI and between TEL3 and NAI are, respectively, 168 and 127° .

In order to test and calibrate the particle telescopes, single-particle inclusive cross sections were measured in TEL2 and TEL3. We compare our results to the data of Sandoval et al.⁽¹⁸⁾ at the same incident energy of 2.1 GeV per nucleon using a scaling factor $A_p^{2/3} A_t$, where A_p and A_t are the projectile and target atomic numbers, respectively.

Fig. 2 refers to the cross sections measured in TEL2. For proton production, it is seen that our results are in good agreement, in magnitude and shape, with the data of Sandoval et al. For deuterons, the agreement is also good. We do not have an absolute normalization for the single-particle cross-sections measured in TEL3. Fig. 3 gives our results in arbitrary units. They are seen to agree quite well in shape with Sandoval et al. data, for both protons and deuterons.

III. GAMMA-RAY SPECTRA AND THEIR ANALYSIS

III.1) Gamma ray spectra

Gamma-ray spectra have been extracted for both C and Pb targets, using both TEL2·NAI and TEL3·NAI coincidence requirements, and the three following conditions on the particle telescope sides :

Condition 1 : anything in the particle telescopes satisfying the coincidence requirement (this includes particles which are absorbed in the telescopes as well as punch through particles)

Condition 2 : protons in the particle telescopes (30–120 MeV for TEL2, 60–200 MeV for TEL3)

Condition 3 : deuterons in the particle telescopes (40–180 MeV for TEL2, 80–300 MeV for TEL3).

The most inclusive measured γ -ray cross sections are those under condition 1. For conditions 2 and 3, the energy spectra of the charged particles were also extracted, and the invariant mass distributions computed on an event-by-event basis (see next section). Due to low statistics, conditions 2 and 3 were not used for TEL2 when the target was ^{12}C .

Fig. 4 shows examples of the laboratory frame γ -ray spectra. The efficiency of the NAI detector as a function of the gamma energy has been accounted for, but the resolution has not. The solid lines are exponential fits to the spectra above 90 MeV, using the form $k \exp(-E_\gamma/T)$, where k and T are the normalization and slope parameters. Table I gives the values of T and k for these data. The parameter T does not seem to depend much on the type of condition, except perhaps for condition 3, where we have a lower value for Pb and a higher one for C (with large errors). This apparent constancy of T suggests that there is little or no correlation between the gamma detected on one side and the particle on the other side. In addition, we observe no obvious sharp lines or bumps in the γ -ray spectra. Our T values are consistent with Budiansky⁽³⁾ measurements, which for a central trigger were :

$$T = 175 \text{ MeV for Ar (1.8 GeV/A) + Pb} \rightarrow \gamma(30^\circ)$$

$$T = 70 \text{ MeV for Ar (1.8 GeV/A) + Pb} \rightarrow \gamma(90^\circ)$$

$$T = 176 \text{ MeV for Ne (2.1 GeV/A) + Pb} \rightarrow \gamma(30^\circ)$$

$$T = 76 \text{ MeV for Ne (2.1 GeV/A) + Pb} \rightarrow \gamma(90^\circ)$$

the error on these numbers being 5 MeV.

III.2) Number of π^0 's per trigger

We define the "number of γ 's per trigger" as the quantity n_γ computed from :

$$n_\gamma = 4\pi\sigma_\gamma/\sigma_{\text{part}}$$

where σ_γ is the cross section integrated over energy for detecting a γ -ray in coincidence with a particle in one of the telescopes, and σ_{part} is the inclusive cross section integrated over energy for detecting the same particle in the telescopes (this definition assumes isotropic emission of the γ -ray's and negligible particle- γ correlations). We also define the "number of π^0 's per trigger" as :

$$n_{\pi^0} = n_\gamma/2$$

σ_γ is obtained from our measured spectra such as those given in Fig. 4. For condition 1 and TEL2, σ_{part} has been computed from the single particle counting rates (for TEL3, we do not have an absolute normalization). For conditions 2 and 3, σ_{part} has been computed from the data of Sandoval et al.⁽¹⁸⁾, by integration of $d\sigma/dE d\Omega$ over the proper energy range, interpolation between 30 and 50°, and extrapolation using the scaling factor $A_p^{2/3} A_t$ defined above (we note that use of the single-particle cross sections given in Fig. 2 for TEL2 yields similar results). Table 2 shows our n_{π^0} numbers, along with those given by Hallman⁽²⁾ and values computed from Budiansky's thesis⁽³⁾. It is seen from the table that n_{π^0} is about 2 to 4 times larger for the lead target than for carbon. Because of the given statistical errors and a systematical error of the order of 20%, we do not think that the factor 2 difference in rates for TEL2 and TEL3 triggers is meaningful. Finally, comparison of our measured numbers to Hallman's and Budiansky's suggests that our data are mainly related to peripheral collisions (assuming negligible particle-gamma correlations).

III.3) π^0 inverse exponential slope

If it is assumed that in the nucleon-nucleon center of mass frame (CM) an isotropic π^0 energy distribution is of the form:

$$\frac{1}{p'} \frac{d\sigma}{dE'} = k_0 e^{-E'/T_0}$$

where p' and E' are the CM momentum and kinetic energy, respectively, and k_0 and T_0 are parameters (we'll refer to T_0 as the " π^0 inverse exponential slope" or simply "inverse slope"), Budiansky⁽³⁾ shows that the CM gamma energy spectra are given by :

$$\frac{d\sigma}{dE'_\gamma} = 2k_0 T_0 \exp \left[-\frac{1}{T_0} \left(\frac{m^2}{4E'_\gamma} + E'_\gamma - m \right) \right]$$

where E'_γ is the CM gamma energy and m the pion mass. We get the laboratory gamma energy distribution from this last equation as :

$$\frac{d\sigma}{dE_\gamma} = 2 \frac{1}{\alpha} k_0 T_0 \exp \left[-\frac{1}{T_0} \left(\frac{m}{4\alpha E_\gamma} + \alpha E_\gamma - m \right) \right] \quad (1)$$

in which E_γ is the laboratory gamma energy and

$$\alpha = \gamma(1 - \beta \cos \theta)$$

where θ is the laboratory gamma emission angle, β is the speed of the CM frame in the laboratory and γ the corresponding Lorentz factor.

Expression (1) fits our data (see Fig. 5). Table 3 gives the parameters T_0 and k_0 . The π^0 inverse slope does not depend strongly on the type of trigger (as already shown for T in Table I). Under condition 3 (deuterons), it seems to be smaller for the lead target and larger for carbon. Also given in the table, for both targets, are the inverse slopes averaged over all conditions. Table 4 shows the π^0 inverse slope as a function of the CM photon emission angle θ_{CM} . We have given our numbers averaged over all conditions, along with numbers from Budiansky⁽³⁾ and Budiansky et al⁽⁴⁾. Even if the triggers were not the same in both experiments and the detector resolutions have not been corrected for, the measured values are consistent. It is seen that there is little dependence on the projectile mass number and only a slight dependence on the target mass number (T_0 higher for lower masses), and that the inverse slope increases with the angle above 90° CM, giving indications of forward/backward peaking in the angular distribution (as already mentioned in ref. 3).

IV. INVARIANT MASS DISTRIBUTIONS AND THEIR ANALYSIS

IV.1) Invariant mass distributions

The invariant mass distributions have been computed on an event-by-event basis, for TEL3 NAI events only, due to the lack of statistics for TEL2·NAI events. Energy and angle resolutions have not been included in the calculation. Fig. 6 shows the experimental results. The energy bin widths have been chosen more or less empirically, taking into account the counting rate in each bin. The vertical error bars are statistical only. Within the statistical uncertainties, the distributions do not exhibit any special structure, i.e., sharp lines or bumps.

Assuming no correlations between detected γ -rays and particles, we have done a simulation of these distributions by incoherently throwing in the computer a particle energy E with the probability density $f(E)$, a gamma energy E_γ with the probability density $g(E_\gamma)$, and computing the invariant mass of the gamma-particle system. The simulated distributions have been normalized afterwards to the experimental ones. The function $f(E)$ was obtained by fitting Sandoval et al.⁽¹⁸⁾ data with the expression

$$f(E) \propto \exp(-E/T_p)$$

where T_p is a parameter, as shown on Fig. 7a and c. From Fig. 7b and d, it can be seen that the shapes of our coincident particle energy spectra are consistent with the exponential behaviour of Sandoval et al. On the gamma side (and for the purposes of this simulation), we have fitted the most inclusive γ -ray spectra in a simple way, using the function :

$$g(E_\gamma) = k \exp\left[(-E_\gamma/T) - \exp(-E_\gamma/T_\ell)\right] \quad (2)$$

in which k and T are the parameters previously computed and T_ℓ a third parameter required to fit the low energy part of the spectra. The values of T_ℓ obtained for the most inclusive condition 1, and both targets, are listed in Table 5, along with k and T . Fig. 8 shows an example of the fit. The results of the simulation calculations are indicated on Fig. 6 (solid lines). They agree quite well with the experimental points, within the error bars which are quite large, especially for the carbon target. Trying to improve the graphical representation, we display in Fig. 9 the ratio of the experimental invariant mass cross section to the simulated one. As before, these plots do not show any significant deviation between experiment and the combinatorics based simulation.

IV.2) Limits on cross sections for producing anomalons

We consider an object (anomalon) which decays into particle(s) and a gamma-ray. As stated in the introduction, we look for singly charged anomalous fragments, that are labelled below as d^* , and we investigate the simple decay modes:

$$d^* \rightarrow d + \gamma \quad (3)$$

$$d^* \rightarrow (pn) + \gamma \quad (4),$$

i.e., anomalons going to deuteron ground-states or to unbound proton-neutron systems, in this latter case both proton and neutron being emitted with no relative momentum. The more general decay mode into the three-body final state $p + n + \gamma$ is not taken into account because it would not produce any peaks in the experimental spectra. Defining M_a as the mass of d^* and M_{inv} the d - γ or p - γ invariant masses, we have:

$$M_{inv} = M_a \quad \text{for decay channel} \quad (3)$$

$$M_{inv}^2 = \frac{1}{2} M_a^2 - m_p^2 \quad \text{for decay channel} \quad (4)$$

where m_p is the proton mass.

The measured invariant mass cross sections are:

$$\sigma_{EXP} = \int \frac{d\sigma}{dM_{inv} d\Omega_\gamma d\Omega} \quad dM_{inv} \approx \frac{d\sigma}{dM_{inv} d\Omega_\gamma d\Omega} \Delta M_{inv} \approx \frac{d\sigma}{d\Omega_\gamma d\Omega}$$

where $d\Omega_\gamma$ and $d\Omega$ are the elements of solid angles in the directions of the photon and particle (p or d) momenta, respectively. As an example, the limits on the cross sections for producing an anomalon of mass 2176 MeV (≈ 2200 MeV) decaying into $d + \gamma$ is obtained from Fig. 6c and d by taking two standard deviations of the cross sections and multiplying by the mass bin width $\Delta M_{inv} = \Delta M = 100$ MeV:

$$\sigma_{EXP} = .03 \times 100 = 3.0 \text{ mb/sr}^2 \text{ for C + Pb}$$

$$\sigma_{EXP} = .002 \times 100 = 0.2 \text{ mb/sr}^2 \text{ for C + C.}$$

In the same way, we have extracted from the data the limits on the cross section for producing anomalons of masses 2076 and 2276 MeV, respectively. The numbers are listed on Table 6, for both decay channels under consideration. We proceed now to extract the anomalon production cross section $d\sigma/d\Omega_a$ in the laboratory frame by taking into account the detection acceptance.

There are five independent variables that we can choose :

- E_a , the anomalon kinetic energy in the laboratory frame,
- Ω_a , the solid angle which includes both polar and azimuthal emission angles of the anomalon in the laboratory frame,
- Ω'' , the solid angle including both polar and azimuthal emission angles of the γ -ray in the anomalon rest frame.

Thus, we start with the totally differential cross section $d\sigma/dE_a d\Omega_a d\Omega''$ and get the measured cross sections of gamma-particle events with a particle kinetic energy E in the range ΔE , the photon being detected in the NAI solid angle $\Delta\Omega_\gamma$, and the particle in the TEL3 solid angle $\Delta\Omega$, as :

$$\begin{aligned}\sigma_{\text{EXP}} &= \frac{d\sigma}{d\Omega_\gamma d\Omega} = \\ &= \frac{1}{\Delta\Omega_\gamma \Delta\Omega} \int_{\Delta E} \int_{\Delta\Omega_\gamma} \int_{\Delta\Omega} \frac{d\sigma}{dE_a d\Omega_a d\Omega''} \frac{\partial E_a \partial \Omega_a \partial \Omega''}{\partial E \partial \Omega_\gamma \partial \Omega} dE d\Omega_\gamma d\Omega\end{aligned}$$

Since we do not know $d\sigma/dE_a d\Omega_a d\Omega''$, we have made calculations under the reasonable assumption that it is isotropic over $\Delta\Omega''$ and over the small solid angle range $\Delta\Omega_a$ defined by the experimental acceptance $\Delta E - \Delta\Omega_\gamma - \Delta\Omega$, and exponential with respect to E_a , i.e., we take :

$$\frac{d\sigma}{dE_a d\Omega_a d\Omega''} = k_a e^{-E_a/T_a}$$

k_a and T_a being constants. Introducing the detection acceptance factor :

$$A_C(\Delta E, \Delta\Omega_\gamma, \Delta\Omega) = \frac{\int_{\Delta E} \int_{\Delta\Omega_\gamma} \int_{\Delta\Omega} e^{-E_a/T_a} \frac{\partial E_a}{\partial E} \frac{\partial \Omega_a}{\partial \Omega_\gamma} \frac{\partial \Omega''}{\partial \Omega} dE d\Omega_\gamma d\Omega}{\int_{\Delta E_a} e^{-E_a/T_a} dE_a}$$

we then get the convenient anomalon cross section $d\sigma/d\Omega_a$, which will be compared to the corresponding deuteron cross section, by integration of $d\sigma/dE_a d\Omega_a d\Omega''$ over $4\pi(\Omega'')$ and over ΔE_a defined by the experimental acceptance, and by elimination of k_a in the calculation :

$$\frac{d\sigma}{d\Omega_a} = \sigma_{EXP} \frac{4\pi \Delta\Omega_\gamma \Delta\Omega}{A_C(\Delta E, \Delta\Omega_\gamma, \Delta\Omega)}$$

The cross section $d\sigma/d\Omega_a$ can be computed using this last expression once we have decided on a reasonable value of the slope parameter T_a . We have made the assumption that T_a is equal to the measured value for deuterons, at the same average emission angle $\langle \theta_a \rangle$. From the data of Sandoval et al.⁽¹⁸⁾, we obtained $T_a = 103$ MeV. In addition, we have checked that varying T_a from half the above value to infinity does not change the results significantly.

The acceptance factor $A_C(\Delta E, \Delta\Omega_\gamma, \Delta\Omega)$ has been computed using a Monte Carlo method. We distribute events in the ranges $\Delta E_a - \Delta\Omega_a - \Delta\Omega''$ with the probability distribution $dN/dE_a d\Omega_a d\Omega'' = N_0 \exp(-E_a/T_a)$ and check if E falls in the range ΔE , Ω_γ in $\Delta\Omega_\gamma$ and Ω in $\Delta\Omega$. The number of detected events is then:

$$N_{DET} = N_0 \int_{\Delta E} \int_{\Delta\Omega_\gamma} \int_{\Delta\Omega} e^{-E_a/T_a} \frac{\partial E_a}{\partial E} \frac{\partial \Omega_a}{\partial \Omega_\gamma} \frac{\partial \Omega''}{\partial \Omega} dE d\Omega_\gamma d\Omega$$

The total number of throws is :

$$N = N_0 \iiint e^{-E_a/T_a} dE_a d\Omega_a d\Omega''$$

We then have :

$$A_c(\Delta E, \Delta\Omega_\gamma, \Delta\Omega) = \frac{N_{DET}}{N} \Delta\Omega_a \Delta\Omega''$$

giving :

$$\frac{d\sigma}{d\Omega_a} = \sigma_{EXP} \frac{4\pi \Delta\Omega_\gamma \Delta\Omega}{\Delta\Omega_a \Delta\Omega''} \frac{N}{N_{DET}} \quad (5)$$

The kinematical quantities $\langle \theta_a \rangle$, $\Delta\Omega_a$, $\Delta\Omega''$ and ΔE_a given by the Monte Carlo calculation are shown in Table 7, and the values of $d\sigma/d\Omega_a$ obtained from equation (5) are given in Table 8.

For better interpretation, we compare the above cross section limits to deuteron production cross sections in the same kinematical energy range ΔE_a and at the same average scattering angle $\langle \theta_a \rangle$. The latter are computed from the data of Sandoval et al.⁽¹⁸⁾ (Ne + U at 2.095 GeV per nucleon incident energy), using as before the scaling factor $A_p^{2/3} A_t$ and integrating over ΔE_a . These deuteron production cross sections, labelled $(d\sigma/d\Omega_a)_d$, are listed on Table 8. Now, we can compare anomalon production rates to those of deuterons by using the ratio of the corresponding cross sections computed under the same kinematical conditions :

$$n = \frac{d\sigma/d\Omega_a}{(d\sigma/d\Omega_a)_d} .$$

These ratios, expressed in percentage, are also listed in Table 8. It is seen that the computed rate limits are almost independent of the target Pb or C. For anomalon masses from 200 to 400 MeV above the deuteron mass, our experiment sets the limits on anomalon production rates from 2 to 10% of the deuterons for the decay channel (3), and 5 to 20% for the decay channel (4).

IV.3) Lifetime effect on our measurements

We have investigated a possible lifetime effect for anomalons on our invariant mass measurements in the following simple way.

Let \vec{R}_Y and \vec{R} be the vector radii defining the NAI and TEL3 detector positions from the target center. If anomalous decay after a path \vec{r} , γ -rays and deuterons (or protons) would reach the detectors along the vector radii \vec{R}'_Y and \vec{R}' such that $\vec{R}_Y = \vec{r} + \vec{R}'_Y$ and $\vec{R} = \vec{r} + \vec{R}'$. Our measured invariant mass distributions were computed under the assumption of no lifetime effect, i.e., from the expression :

$$M_{\text{comp}}^2 = (E_Y + E)^2 - \left(E_Y \frac{\vec{R}_Y}{R_Y} + p \frac{\vec{R}}{R} \right)^2$$

where E_Y as before is the photon energy, E and p are the total relativistic energy and momentum of the deuteron (or proton) respectively, while the invariant mass squared is given by :

$$M^2 = (E_Y + E)^2 - \left(E_Y \frac{\vec{R}'_Y}{R'_Y} + p \frac{\vec{R}'}{R'} \right)^2$$

From these two expressions, with the approximation $r \ll R_Y$ or R , and introducing the anomalon speed \vec{v} and laboratory mean lifetime t with $\vec{r} = \vec{v}t$, we have:

$$\frac{\Delta M}{M} = \frac{M_{\text{comp}} - M}{M} \approx - \frac{E_Y p}{M^2} t \vec{v} \cdot \vec{G} \quad (6)$$

where the vector \vec{G} is defined by the geometry of the experiment (\vec{R}_Y and \vec{R}):

$$\vec{G} = \frac{\vec{R}_Y}{R_Y^2} \left(\frac{R_Y}{R} - \frac{\vec{R}_Y \cdot \vec{R}}{R_Y R} \right) + \frac{\vec{R}}{R^2} \left(\frac{R}{R_Y} - \frac{\vec{R}_Y \cdot \vec{R}}{R_Y R} \right)$$

E_Y , p and \vec{v} are obtained from the Monte Carlo calculation. We have taken the maximum values of E_Y , p and v and the average values of the angles defining the direction of \vec{v} . The upper limits of the laboratory mean lifetime can be computed using equation (6) once we have decided which ΔM values would wash out characteristic mass peaks or bumps. Choosing ΔM equal to 1/5 of the mass bin widths, we have obtained the mean lifetime upper limits given in Table 9 (the listed numbers refer not to t but to the conventional mean lifetime in the anomalon rest frame). It is seen that these lifetime limits are much larger than the value of 3×10^{-11} s given by Barber et al. (9).

V. CONCLUSION

We have presented results relative to the analysis of γ -ray spectra and invariant mass distributions in carbon-nucleus collisions at 2.1 GeV per nucleon.

The γ -ray spectra exhibit no obvious sharp lines or bumps and little or no correlation with the energy and type of detected particles on the charged particle side. They are interpreted in terms of π^0 inverse exponential slope and production rate. The low numbers of π^0 's per trigger suggest that our data are mostly related to peripheral collisions. The π^0 yield is higher for the lead target than for carbon by a factor of 3 ± 1 . Our measured π^0 inverse slopes are 110 MeV for Pb and 160 MeV for C targets. As a function of the CM γ -ray emission angle, they are in good agreement with the Budiansky⁽³⁾ and Budiansky et al.⁽⁴⁾ results. The inverse slope increases with the CM angle; there is no dependence on the projectile mass number and some dependence on the target mass (higher inverse slopes for lower masses).

The raw particle-gamma invariant mass distributions do not show any unusual structure. They can be well understood from a Monte Carlo calculation that incoherently throws particle and gamma-ray energies with probability densities corresponding to their respective experimental inclusive cross sections. We have computed cross section upper limits for the proposed decay process of singly charged anomalous going to a gamma-ray and a bound deuteron or an unbound proton-neutron system. For anomalous masses in the range 200–400 MeV above the deuteron mass, the upper limits are about 2 to 20% of the deuteron production rate, for both Pb and C targets, these cross section limits being compatible with mean lifetimes up to about 10^{-9} s. Our result is in agreement with Gustafsson et al.⁽¹⁹⁾ experiment which rules out the Barber et al.⁽⁹⁾ decay model up to mean lifetimes of 3×10^{-11} s. Our envisioned process is more specific because it precisely concerns electromagnetic decay with the emission of a single γ -ray, but our lifetime limit is much higher (which comes from the fact that we have studied target fragments instead

of projectile ones). With regard to the model of Friedlander et al.⁽⁷⁾ stating that about 6% of the fragments are anomalous and that their disappearance could be due to depletion by a very large reaction cross section, our production rate limits are too high for significantly ruling out our assumed competing decay process.

ACKNOWLEDGMENTS

We would like to thank the Bevatron crew, particularly Fred Lothrop, Bob Miller, and Jose Alonso, for providing the beam on target. Thanks to Everett Harvey for expert help in getting our computer system up and running. Particular thanks go to Al Smith, for his help with the ^{11}C activation studies used to calibrate our ion chamber.

This work was supported by the Director, Office of Energy Research, Division of Nuclear Physics of the Office of High Energy and Nuclear Physics of the U. S. Department of Energy under Contracts DE-AC03-76SF00098, DE-AS05-76ER04699, DE-AC02-76ER03274 and DE-AT03-81ER40027.

TABLE 1

FIT PARAMETERS OF THE GAMMA CROSS SECTIONS (ABOVE 90 MeV) IN THE LABORATORY FRAME

Tgt	(Condition) Coincident Particle	T(MeV)		k(mb/MeV/sr ²)	
		TEL2·NAI	TEL3·NAI	TEL2·NAI	TEL3·NAI
Pb	(1) anything	63 ± 4	63 ± 3	41 ± 7	41 ± 5
	(2) protons	61 ± 10	62 ± 5	11 ± 5	9 ± 2
	(3) deuterons	50 ± 9	50 ± 6	14 ± 9	6 ± 2
C	(1) anything	79 ± 13	73 ± 6	.6 ± .2	1.3 ± .3
	(2) protons		74 ± 8		.18 ± .06
	(3) deuterons		94 ± 18		.03 ± .015

TABLE 2

NUMBER OF π^0 's PER TRIGGER

REFERENCE	REACTION(a)	TYPE OF TRIGGER	n_{π^0}
This experiment (2.1 GeV/nucleon)	C + Pb	TEL2, condition 1 (anything)	$1.45 \pm .08$
		2 (protons)	$1.5 \pm .2$
		3 (deuterons)	$2.4 \pm .3$
	C + C	TEL2, condition 1 (anything)	$.53 \pm .06$
		2 (protons)	$.44 \pm .11$
		3 (deuterons)	$.47 \pm .13$
	C + Pb	TEL3, condition 2 (protons)	$.91 \pm .05$
		3 (deuterons)	$.94 \pm .07$
	C + C	TEL3, condition 2 (protons)	$.61 \pm .12$
		3 (deuterons)	$.38 \pm .06$
Hallman ⁽²⁾ (2.1 GeV/nucleon)	C + Pb	Low multiplicity cut	$2.6 \pm .2$
		↓	$2.9 \pm .1$
			$3.0 \pm .1$
			$3.4 \pm .2$
		High multiplicity cut	$4.1 \pm .6$
	(1.8 GeV/nucleon) Ar + Pb	Low multiplicity cut	$4.1 \pm .2$
		↓	$4.8 \pm .2$
			$5.4 \pm .2$
			$5.6 \pm .4$
		High multiplicity cut	7.8 ± 1.1
Budiansky ⁽³⁾ (1.8 GeV/nucleon)	Ar + Pb (90°)	central trigger	8.7
	" (30°)	" "	3.4

(a) The γ -ray laboratory emission angle is 124° in our experiment and 90° in Hallman's one. It is 90° and 30° in Budiansky's experiment, as indicated in the table.

TABLE 3

FIT PARAMETERS OF THE GAMMA CROSS SECTIONS USING EXPRESSION (1)

Tgt	(CONDITION) Coincident particle	T_0 (MeV)		k_0 (mb/MeV ² /sr ²)	
		TEL2·NAI	TEL3·NAI	TEL2·NAI	TEL3·NAI
Pb	(1) anything	124 ± 9	123 ± 6	.14 ± .03	.14 ± .02
	(2) protons	122 ± 20	121 ± 9	.04 ± .02	.030 ± .006
	(3) deuterons	100 ± 19	96 ± 11	.05 ± .03	.020 ± .007
	average over all conditions	114 ± 5			
C	(1) anything	158 ± 26	144 ± 11	.0019 ± .0008	.0043 ± .0009
	(2) protons		146 ± 16		.0006 ± .0002
	(3) deuterons		190 ± 38		.00010 ± .00005
	average over all conditions	159 ± 12			

TABLE 4

π^0 inverse exponential slope as a function of the
CM photon emission angle

CM angle (°)	Projectile + target	LAB angle (°)	T_0 (MeV)	Reference
65	Ar + Pb	30	73 ± 5	Budiansky et al ⁽⁴⁾
68	Ne + Pb	30	69 ± 5	"
134	Ar + Ca	90	105 ± 5	"
134	Ar + Pb	90	90 ± 5	"
137	Ne + Pb	90	96 ± 5	Budiansky (3)
156	C + C	124	159 ± 12	This experiment
156	C + Pb	124	114 ± 5	" "

TABLE 5

FIT PARAMETERS OF THE MOST INCLUSIVE γ -RAY SPECTRA USING THE
FIT FUNCTION (2): TEL3-NAI EVENTS

Tgt	k (mb/MeV/sr ²)	T (MeV)	T _g (MeV)
Pb	41	63	22
C	1.3	73	23

Table 6

Experimental limits of the cross sections for producing given invariant masses for both decay modes $d^* \rightarrow d + \gamma$ and $d^* \rightarrow (pn) + \gamma$

Anomalon mass (MeV)	$d^* \rightarrow d + \gamma$		M_{inv} (MeV)	$d^* \rightarrow (pn) + \gamma$	
	σ_{EXP} C + Pb	(mb/sr ²) C + C		σ_{EXP} C + Pb	(mb/sr ²) C + C
2076	.06 X 100 = 6	.003 X 100 = .3	1130	.2 X 50 = 10	.012 X 50 = .6
2176	.03 X 100 = 3	.002 X 100 = .2	1220	.1 X 50 = 5	.008 X 50 = .4
2276	.016 X 100 = 1.6	.001 X 100 = .1	1310	.06 X 50 = 3	.004 X 100 = .4

Table 7

Acceptance of the experimental setup for detecting anomalons (see text for definition of the kinematical quantities)

	Anomalon mass (MeV)	$\langle \theta_a \rangle$ ($^\circ$)	$\Delta\Omega_a$ (sr)	$\Delta\Omega''$ (sr)	ΔE_a (MeV)	N_{DET}/N
$d^* \rightarrow d + \gamma$	2076	47	.21	.27	45-235	.027
	2176	49	.29	.34	35-204	.020
	2276	52	.38	.41	27-174	.016
$d^* \rightarrow (pn) + \gamma$	2076	46	.18	.20	76-320	.035
	2176	47	.24	.26	61-283	.026
	2276	49	.30	.36	46-260	.017

TABLE 8

LIMITS OF CROSS SECTIONS FOR PRODUCING ANOMALONS COMPARED TO DEUTERON PRODUCTION CROSS SECTIONS.

	Anomalon mass (MeV)	$d\sigma/d\Omega_a$ (mb/sr)		$(d\sigma/d\Omega_a)_d$ (mb/sr)		n (%)	
		C + Pb	C + C	C + Pb	C + C	C + Pb	C + C
$d^* \rightarrow d + \gamma$	2076	96	4.8	950	55	10	9
	2176	36	2.4	930	54	3.9	4.5
	2276	14.8	.93	880	51	1.7	1.8
$d^* \rightarrow (pn) + \gamma$	2076	200	12	950	55	21	22
	2176	73	6	970	56	8	10
	2276	38	5	1010	59	4	9

TABLE 9

UPPER LIFETIME LIMITS UNDER WHICH ANOMALON DECAY COULD HAVE BEEN
DETECTED

Anomalon mass (MeV)	Lifetime upper limit (s)
2076	1.8×10^{-9}
2176	1.1×10^{-9}
2276	$.8 \times 10^{-9}$

REFERENCES

- (1) W. DeJarnette et al.
Phys. Lett. 94B, 327 (1980)
- (2) T. Hallman
A study of Central Collisions of Relativistic ^{12}C and ^{40}Ar
on ^{208}Pb , Using Neutral and Charged Pi-Meson Production, and
Charged Particle Multiplicity as Probes
Ph.D. thesis, The Johns Hopkins University (1983), published by
University Microfilms International
- (3) M.P. Budiansky
Measurement of High-Energy Gamma Rays from Relativistic
Heavy-Ion Collisions
Ph.D. thesis, University of California, Berkeley (1981),
unpublished
- (4) M.P. Budiansky et al.
Phys. Rev. Lett. 49, 361 (1982)
- (5) B. Judek
Can. J. Phys. 46, 343 (1968)
- (6) B. Judek
Can. J. Phys. 50, 2082 (1972)
- (7) E.M. Friedlander et al.
Phys. Rev. Lett. 45, 1084 (1980)
- (8) P.L. Jain et al.
Phys. Rev. Lett. 48, 305 (1982)
- (9) H.B. Barber et al.
Phys. Rev. Lett. 48, 856 (1982)

- (10) J. D. Stevenson et al.
Phys. Rev. Lett. 52, 515 (1984)
- (11) T. J. M. Symons et al.
Phys. Rev. Lett. 52, 982 (1984)
- (12) P. L. Jain et al.
Phys. Rev. Lett. 52, 2213 (1984)
- (13) A. P. Gasparian et al.
submitted to the XXII International Conference on High Energy Physics (Leipzig, DDR), to the X International Conference on High Energy Physics and Nuclear Structure (Heidelberg, FRG) and to Zeitschrift für Physik A.
- (14) S. B. Beri et al.
to be published in Physics Letters
- (15) T.M. Liss et al.
Phys. Rev. Lett. 49, 775 (1982)
- (16) S. Frederiksson et al.
5th High Energy Heavy Ion Study, May 18-22 (1981),
LBL-12652, UC-34, CONF-8105104
- (17) In the kinematical region under investigation, Doppler broadening is about two times smaller than the experimental γ energy resolution
- (18) A. Sandoval et al.,
LBL-8771 Preprint (September 1979); Phys. Rev. C21, 1321 (1980)
- (19) H.A. Gustafsson et al.
6th High Energy Heavy Ion Study and 2nd Workshop on Anomalons, June 28-July 1 (1983), LBL-16281

FIGURE CAPTIONS

Fig. 1 – Experimental setup (see text for definition of the abbreviations)

Fig. 2 – The cross sections $d\sigma/dEd\Omega$ measured in TEL2 compared to Sandoval et al. data ⁽¹⁸⁾ using the scaling factor $A^{2/3}A_t$: a) proton cross section; b) deuteron cross section

Fig. 3 – The cross sections $d\sigma/dEd\Omega$ measured in TEL3 compared to Sandoval et al. data ⁽¹⁸⁾: a) proton production; b) deuteron production. Note that the present experiment results are given in arbitrary unit.

Fig. 4 – Examples of γ -ray spectra :
 a) $^{12}\text{C} + \text{Pb}$, TEL2·NAI events, condition 1 (anything)
 b) $^{12}\text{C} + \text{Pb}$, TEL3·NAI events, condition 2 (protons)
 c) $^{12}\text{C} + \text{Pb}$, TEL3·NAI events, condition 3 (deuterons)
 The solid lines are exponential fits (see text)

Fig. 5 – Fit of the spectrum of Fig. 4a using expression (1)

Fig. 6 – Invariant mass distributions for TEL3·NAI events :
 a) Pb target, γ -p invariant mass
 b) C target, γ -p invariant mass
 c) Pb target, γ -d invariant mass
 d) C target, γ -d invariant mass
 The energy cuts on the particle side are : 60–200 MeV for protons, 80–300 MeV for deuterons. The solid lines are from a combinatorics based simulation (see text)

- Fig. 7 - a) Exponential fit of Sandoval et al.⁽¹⁸⁾ data :
 $\text{Ne}(2.095 \text{ GeV/nucleon}) + \text{U} \rightarrow \text{p}(50^\circ)$. The solid line is the fit
 with $T_p = 590 \text{ MeV}$ (see text)
- b) Our experiment (TEL3·NAI events) : $\text{C} + \text{Pb} \rightarrow \text{p} + \gamma$ and
 $\text{C} + \text{C} \rightarrow \text{p} + \gamma$, compared to the above fit.
- c) Exponential fit of Sandoval et al. data :
 $\text{Ne}(2.095 \text{ GeV/nucleon}) + \text{U} \rightarrow \text{d}(50^\circ)$. The solid line is the fit
 with $T_p = 250 \text{ MeV}$ (see text)
- d) Our experiment (TEL3·NAI events) : $\text{C} + \text{Pb} \rightarrow \text{d} + \gamma$ and
 $\text{C} + \text{C} \rightarrow \text{d} + \gamma$, compared to the above fit.

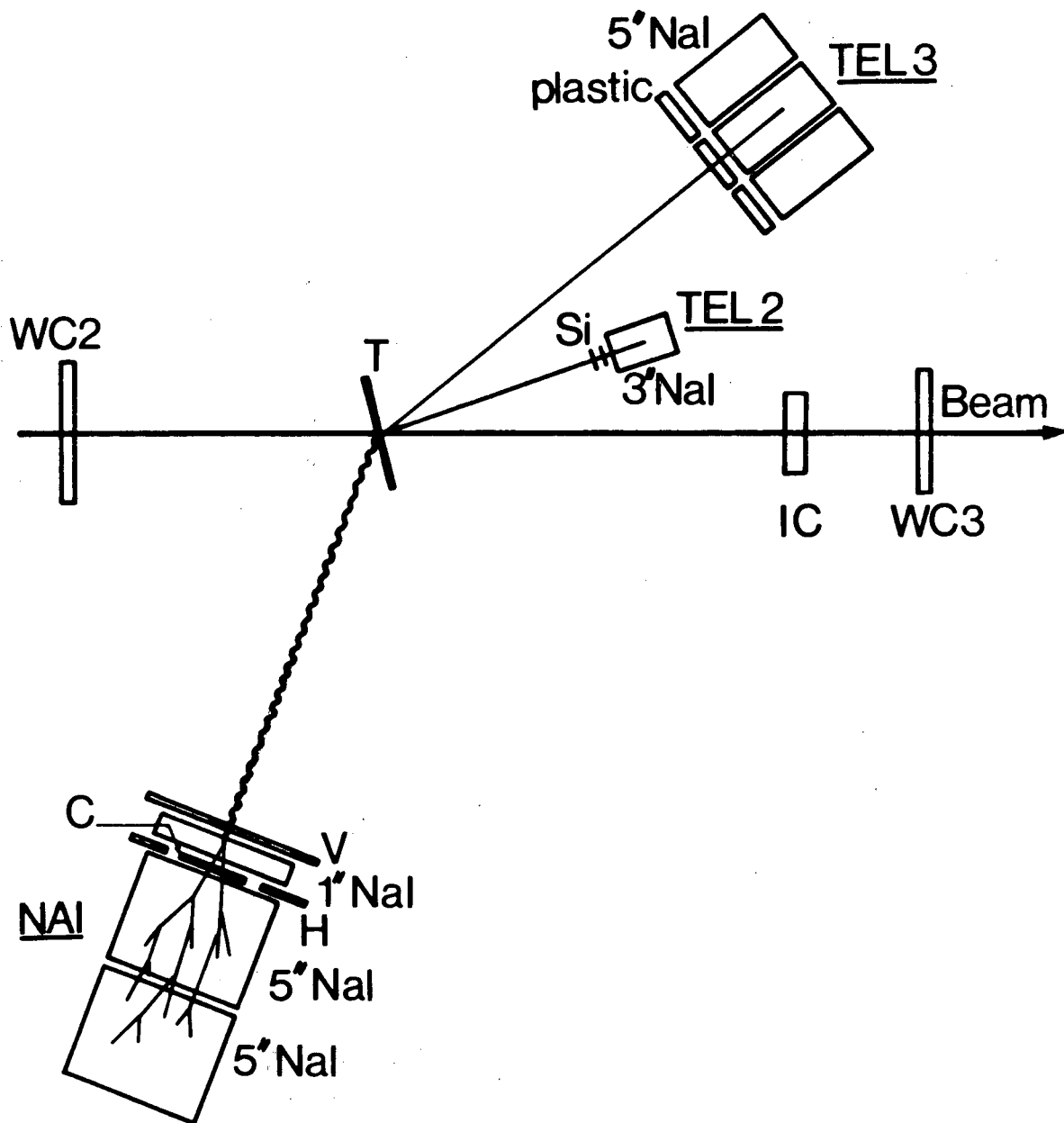
Fig. 8 - Example of fit of a γ -ray spectrum using expression
 (2): $^{12}\text{C} + \text{Pb}$, TEL3·NAI events, condition 1 (anything)

Fig. 9 - Ratio of the experimental gamma-particle invariant mass cross
 over the combinatorics based simulated one, as a function
 of mass.

- a) $\text{C} + \text{Pb} \rightarrow \gamma + \text{p}$
- b) $\text{C} + \text{C} \rightarrow \gamma + \text{p}$
- c) $\text{C} + \text{Pb} \rightarrow \gamma + \text{d}$
- d) $\text{C} + \text{C} \rightarrow \gamma + \text{d}$

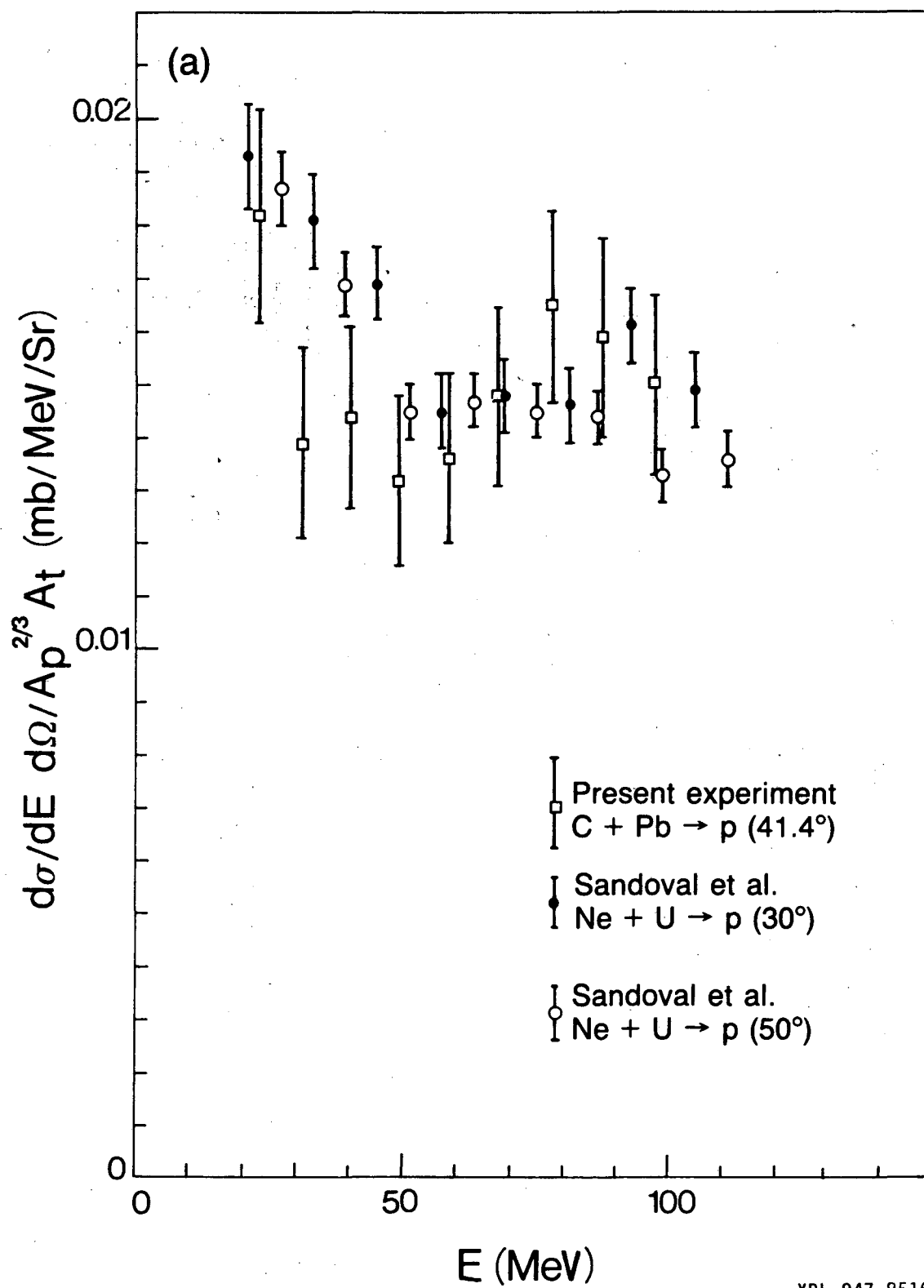
On the vertical axes, the variable is more precisely:

$$d\sigma_{\text{EXP}}/d\sigma_{\text{SIM}} = \left(\frac{d\sigma}{dM d\Omega_\gamma d\Omega} \right)_{\text{EXP}} / \left(\frac{d\sigma}{dM d\Omega_\gamma d\Omega} \right)_{\text{SIM}}$$



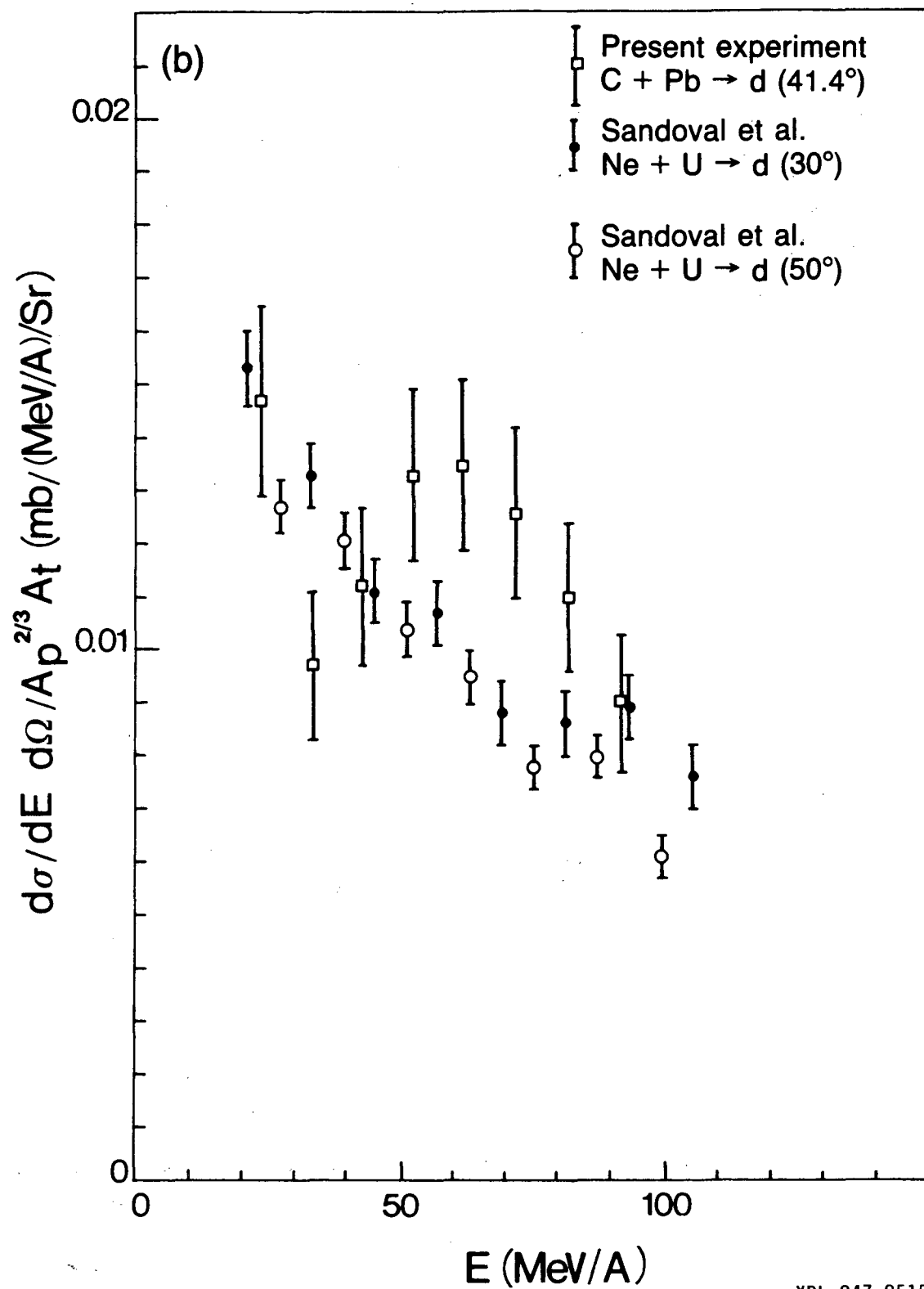
XBL 847-8517

Fig. 1



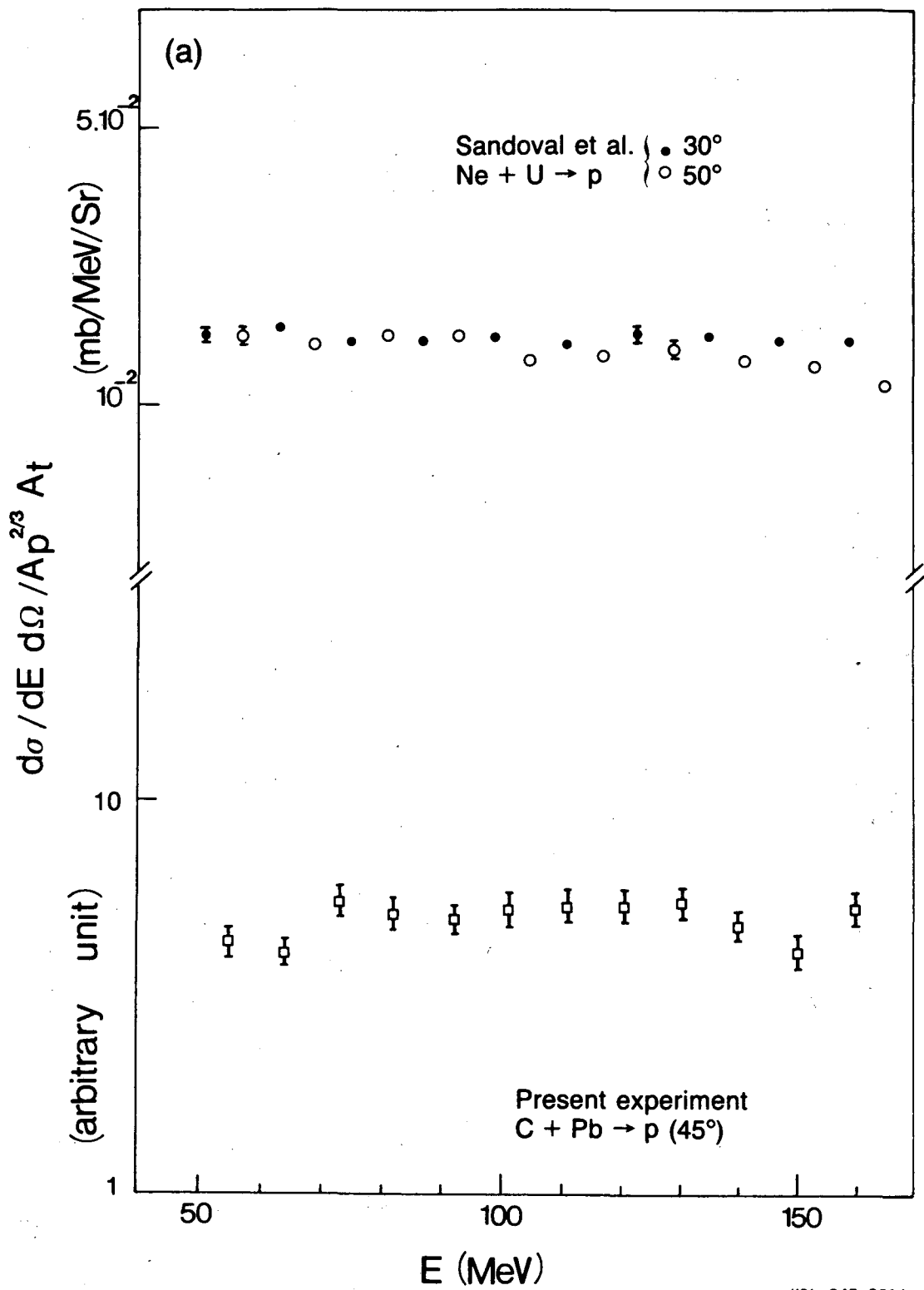
XBL 847-8516

Fig. 2a



XBL 847-8515

Fig. 2b



XBL 847-8514

Fig. 3a

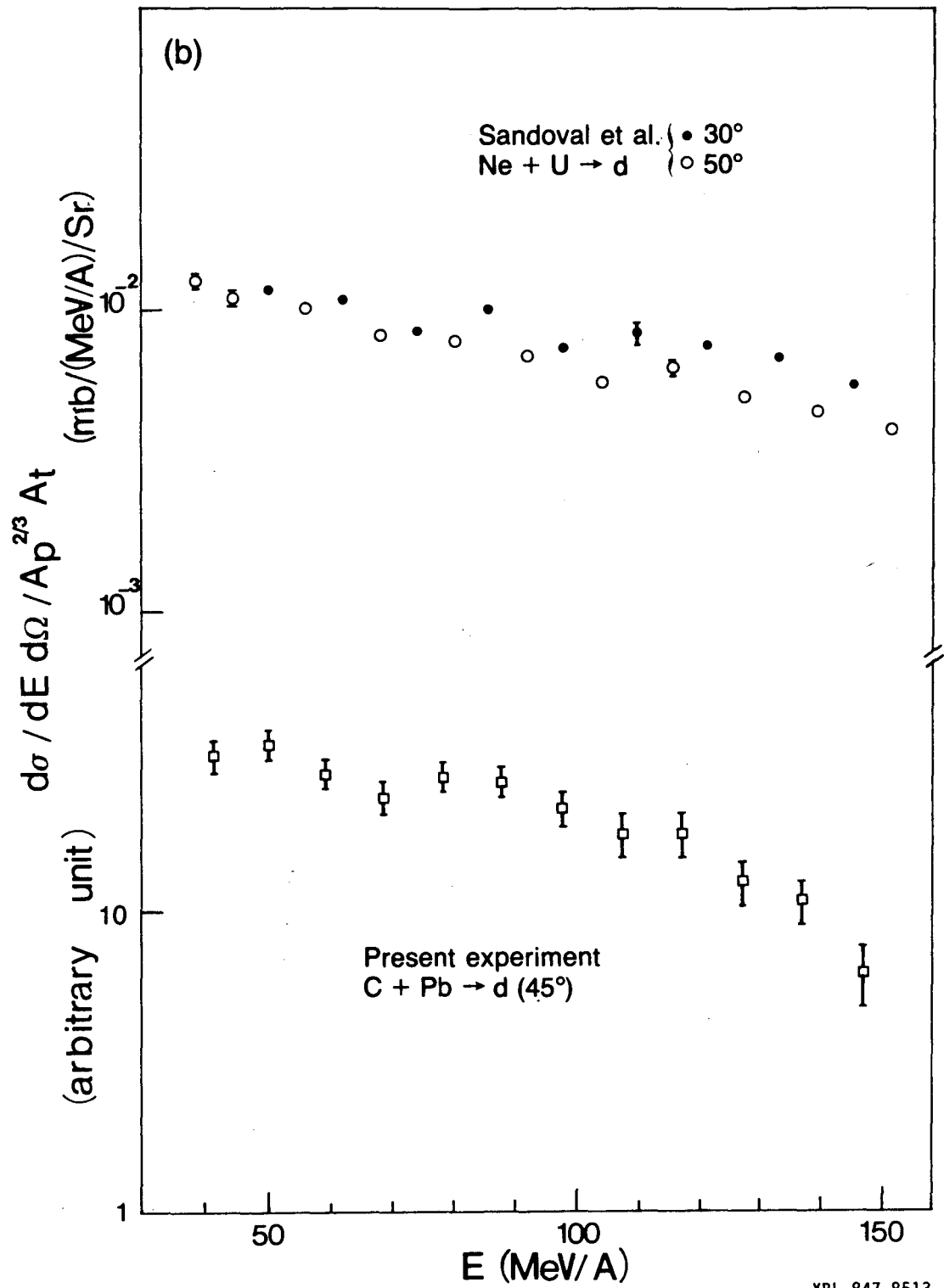


Fig. 3b

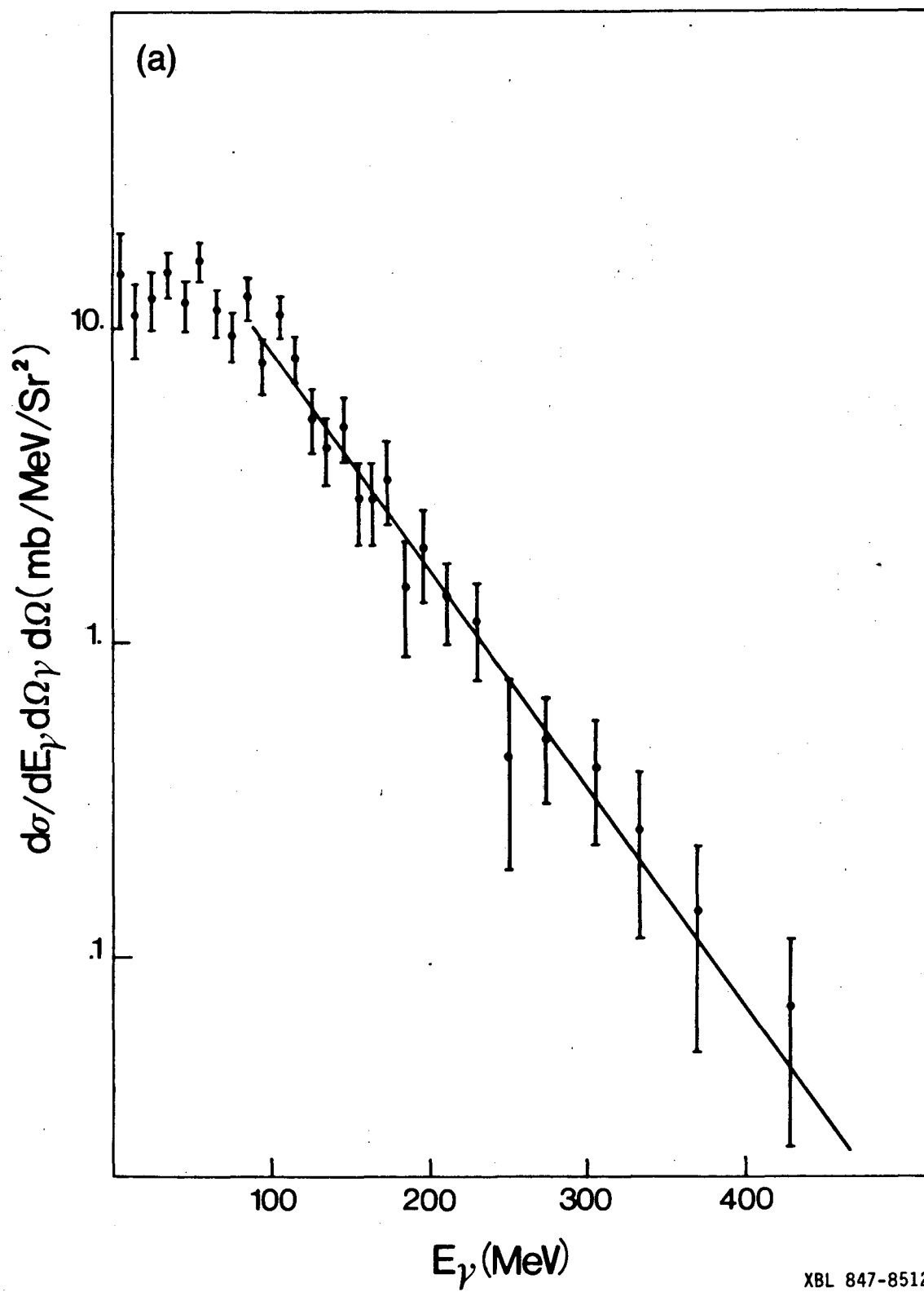


Fig. 4a

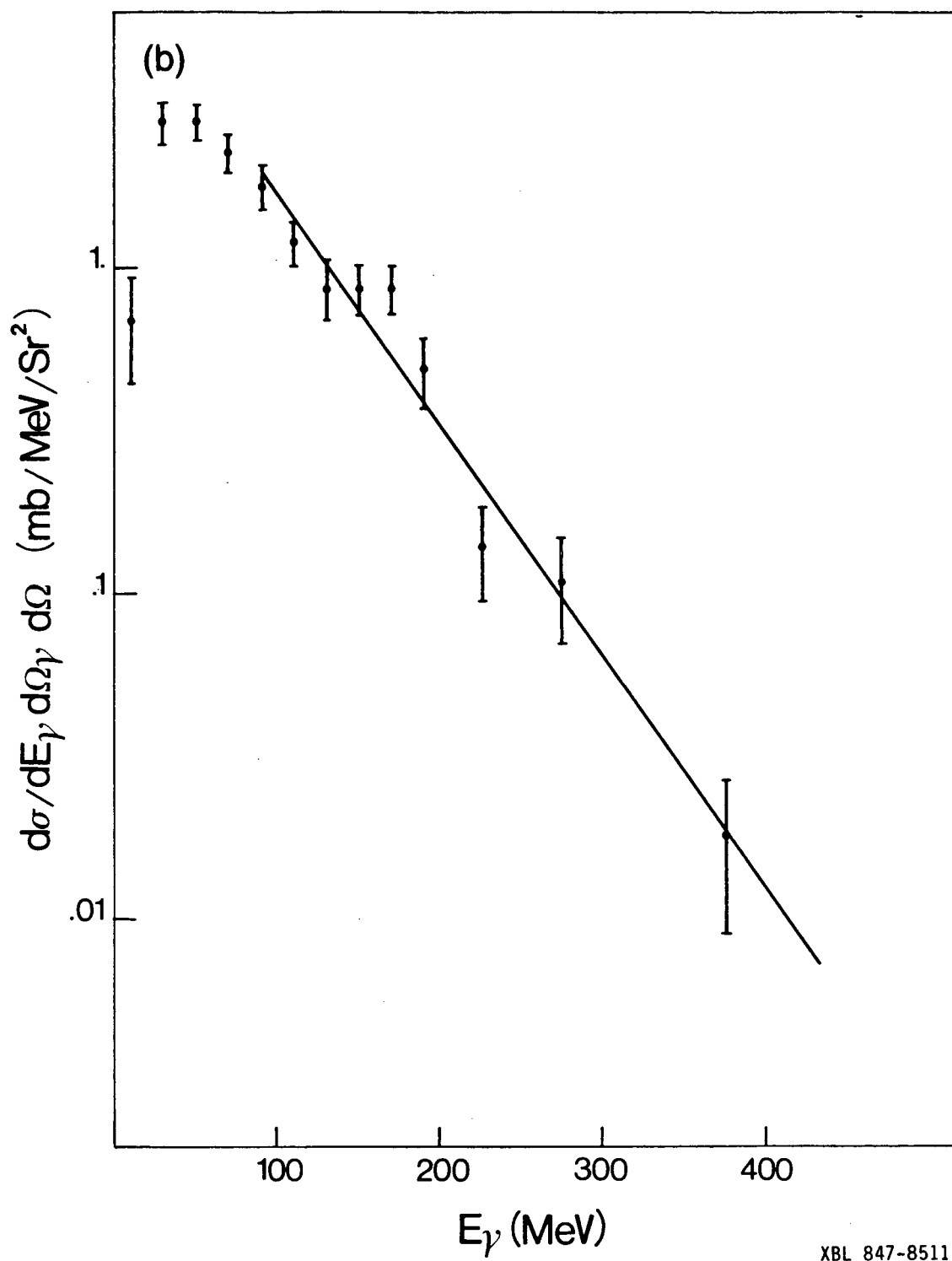
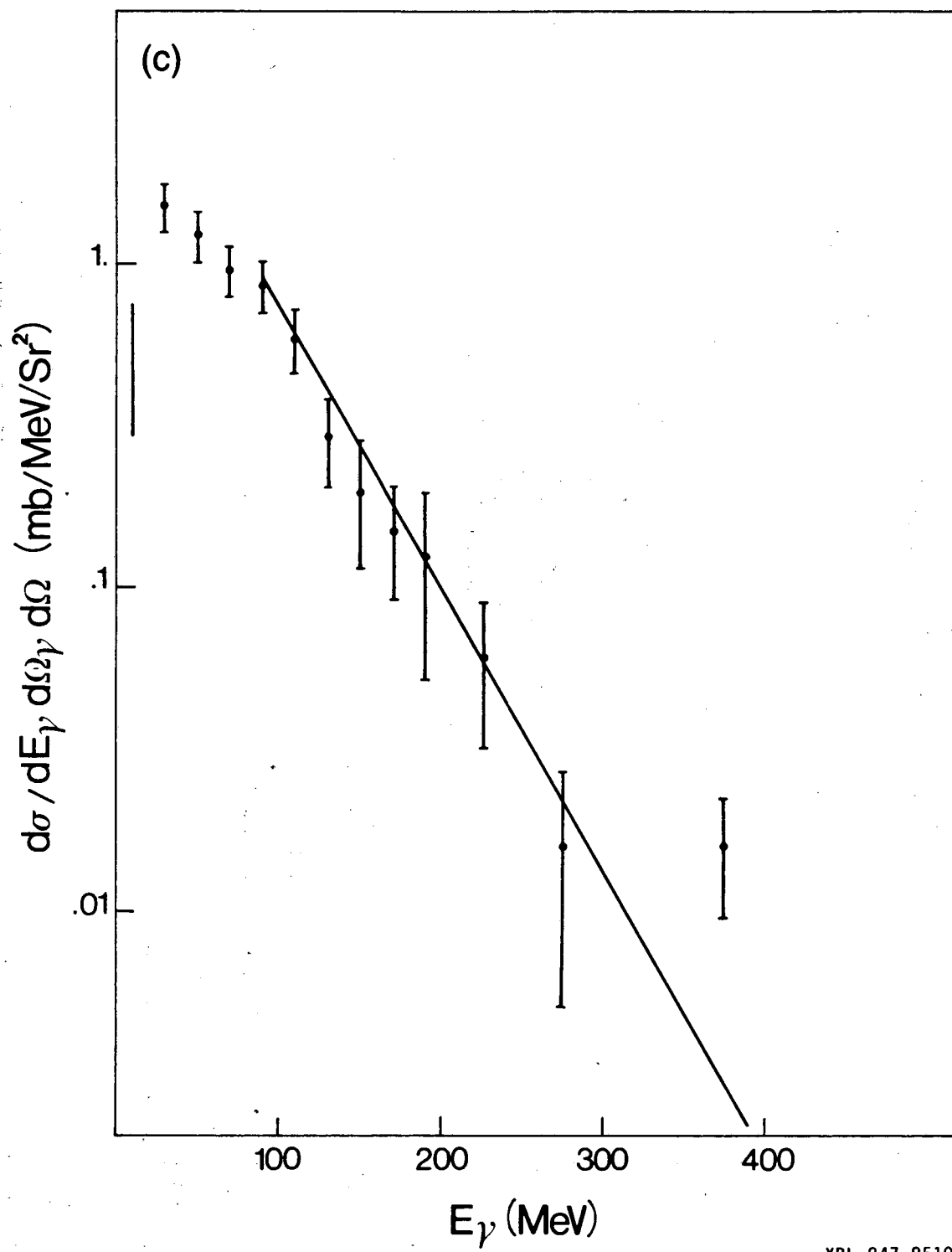
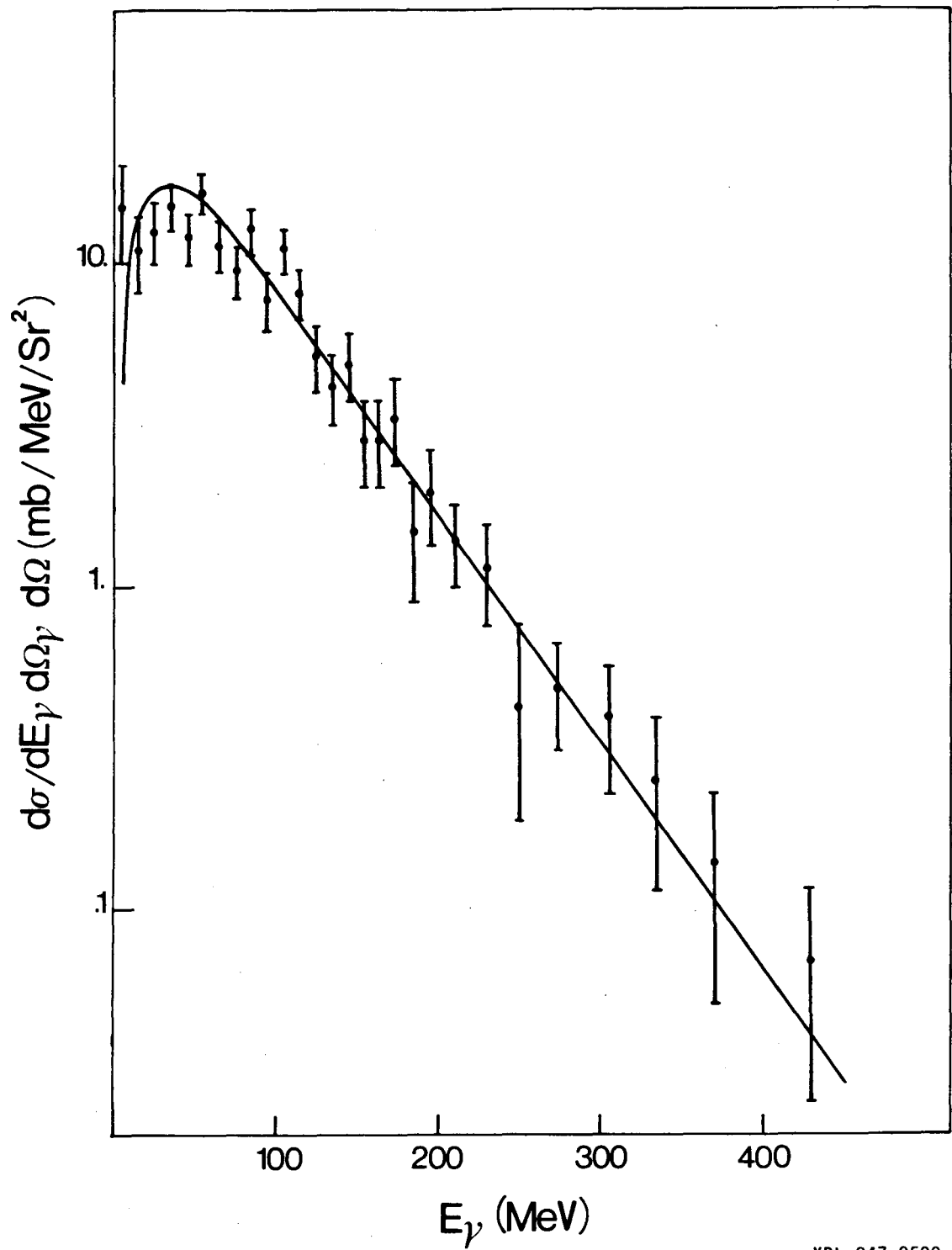


Fig. 4b



XBL 847-8510

Fig. 4c



XBL 847-8509

Fig. 5

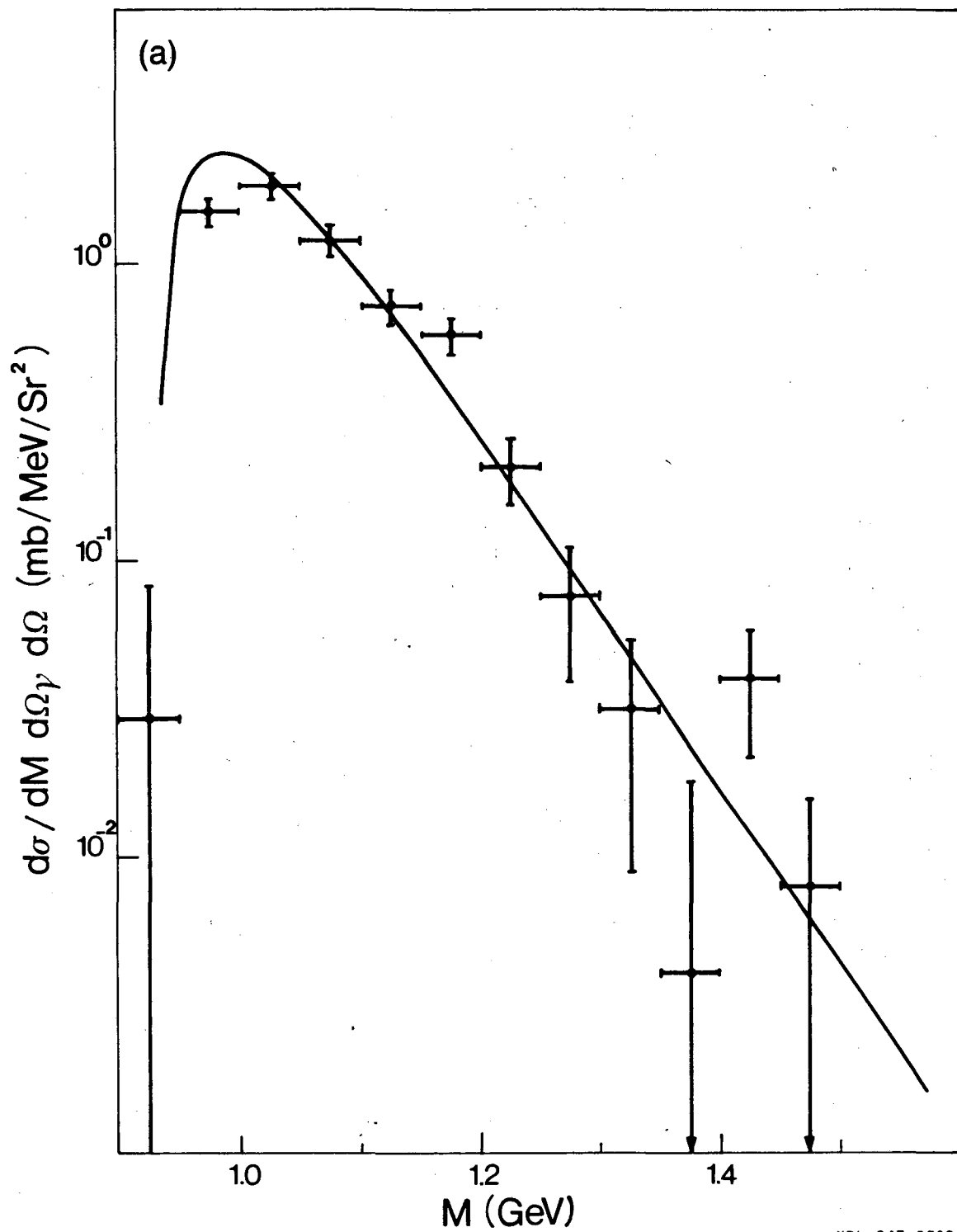
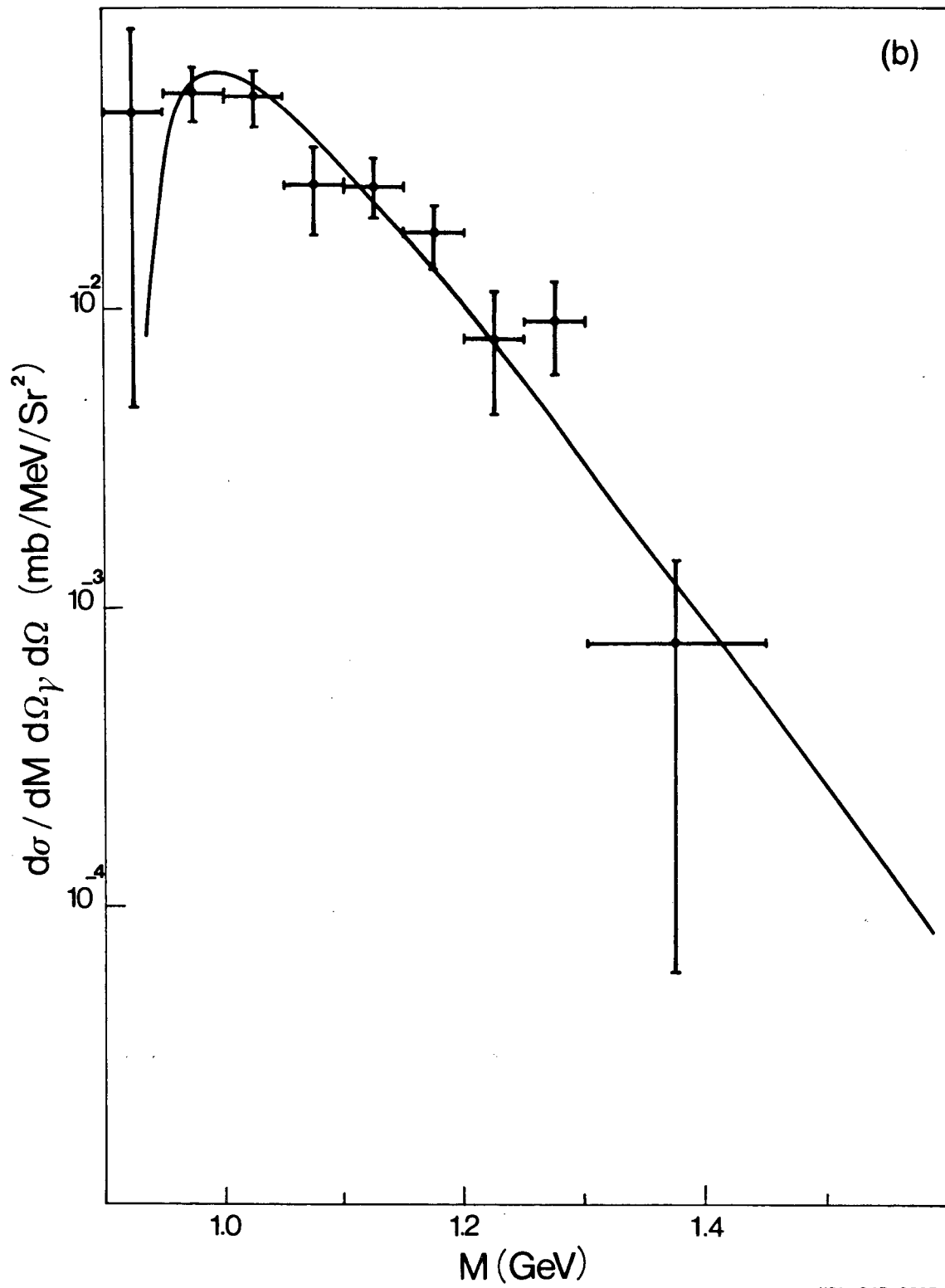
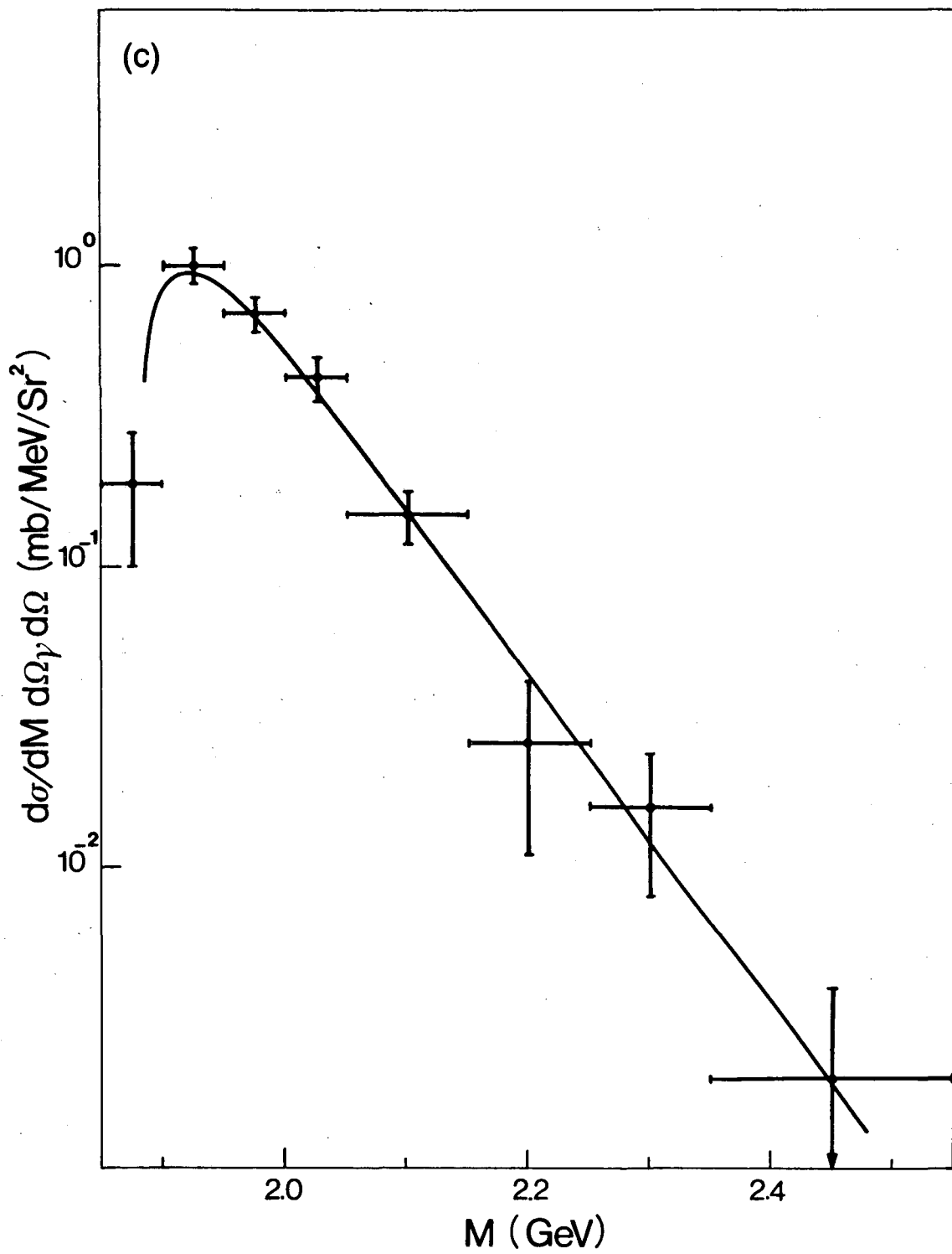


Fig. 6a



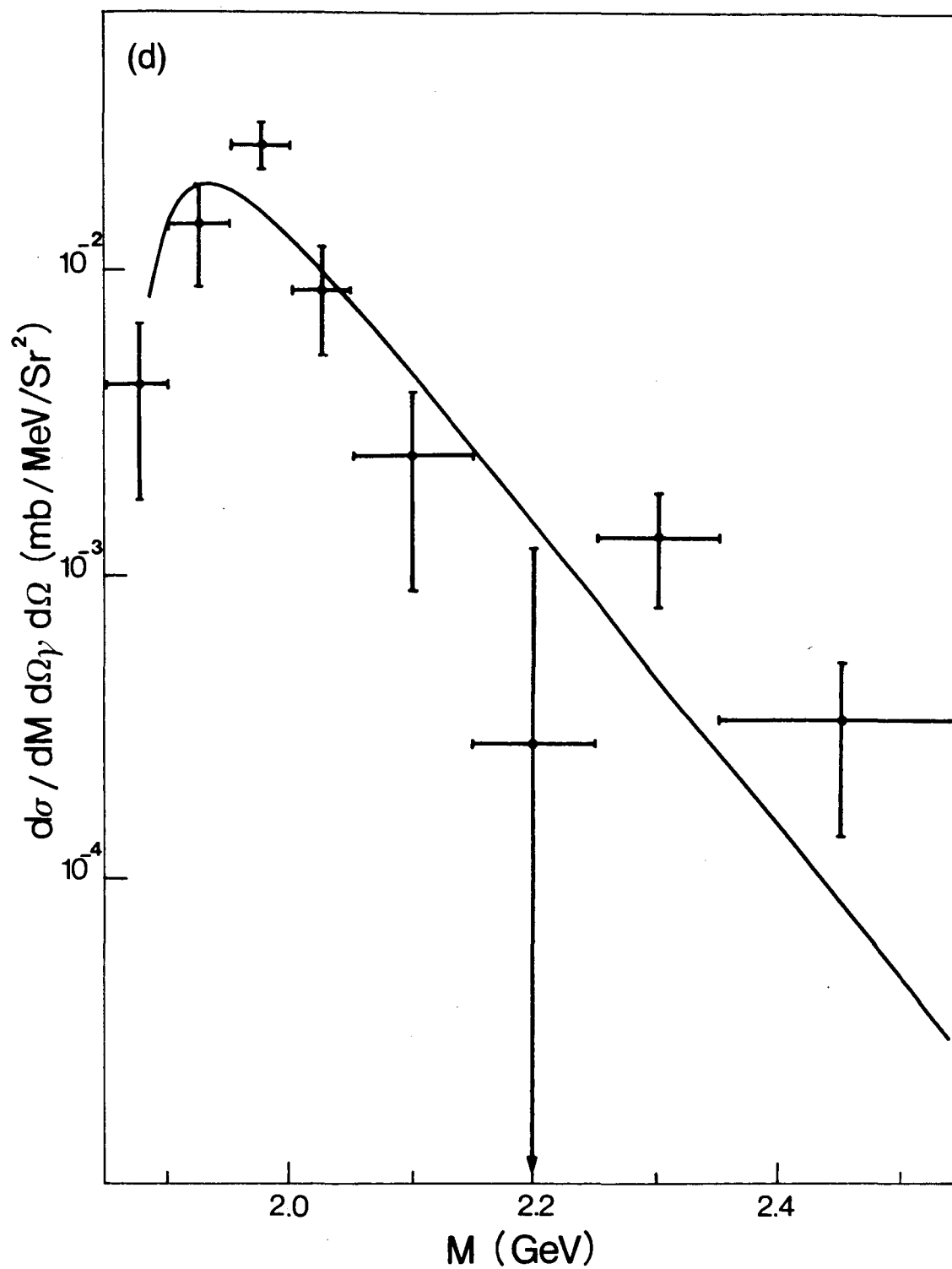
XBL 847-8507

Fig. 6b



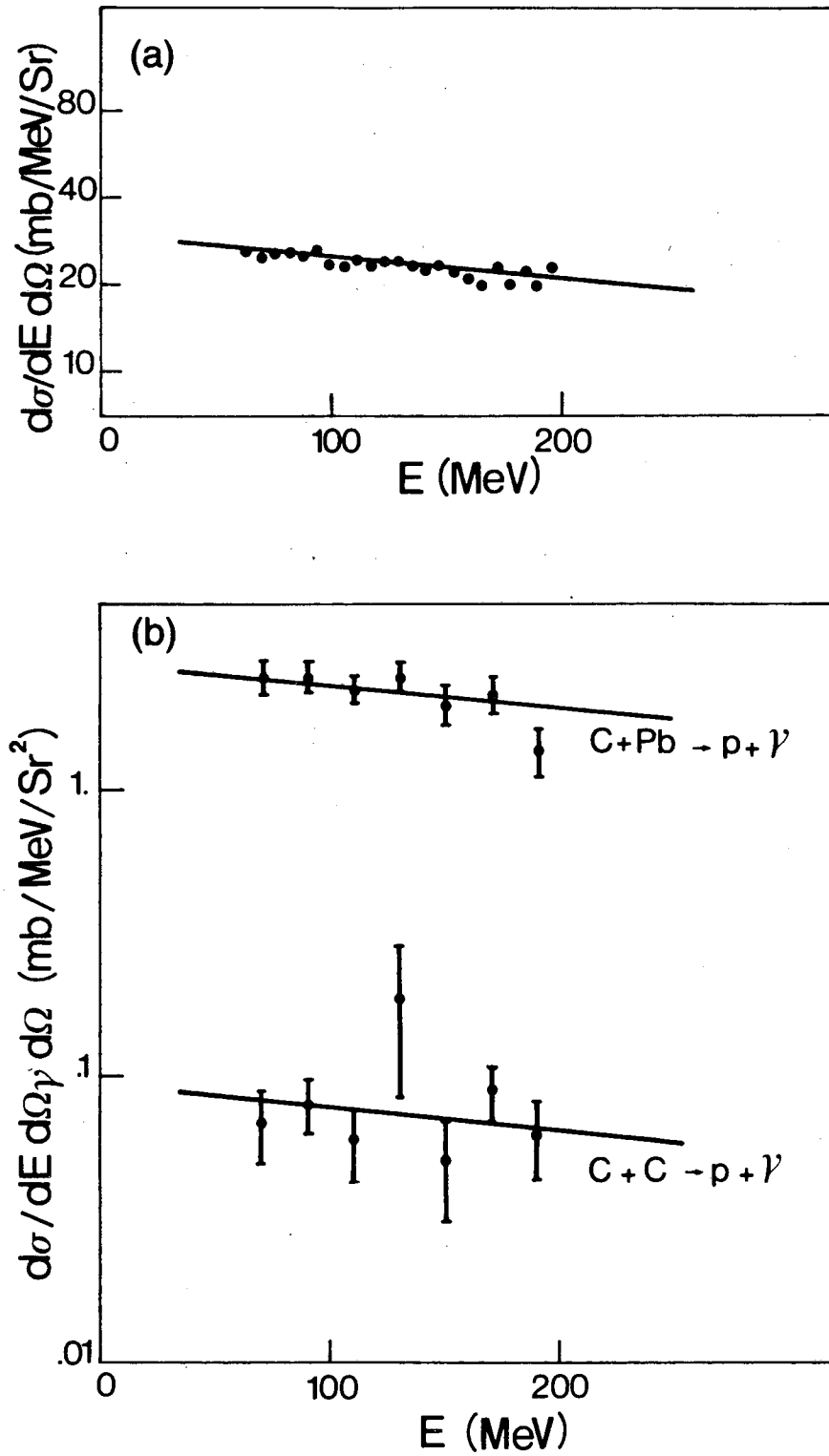
XBL 847-8506

Fig. 6c



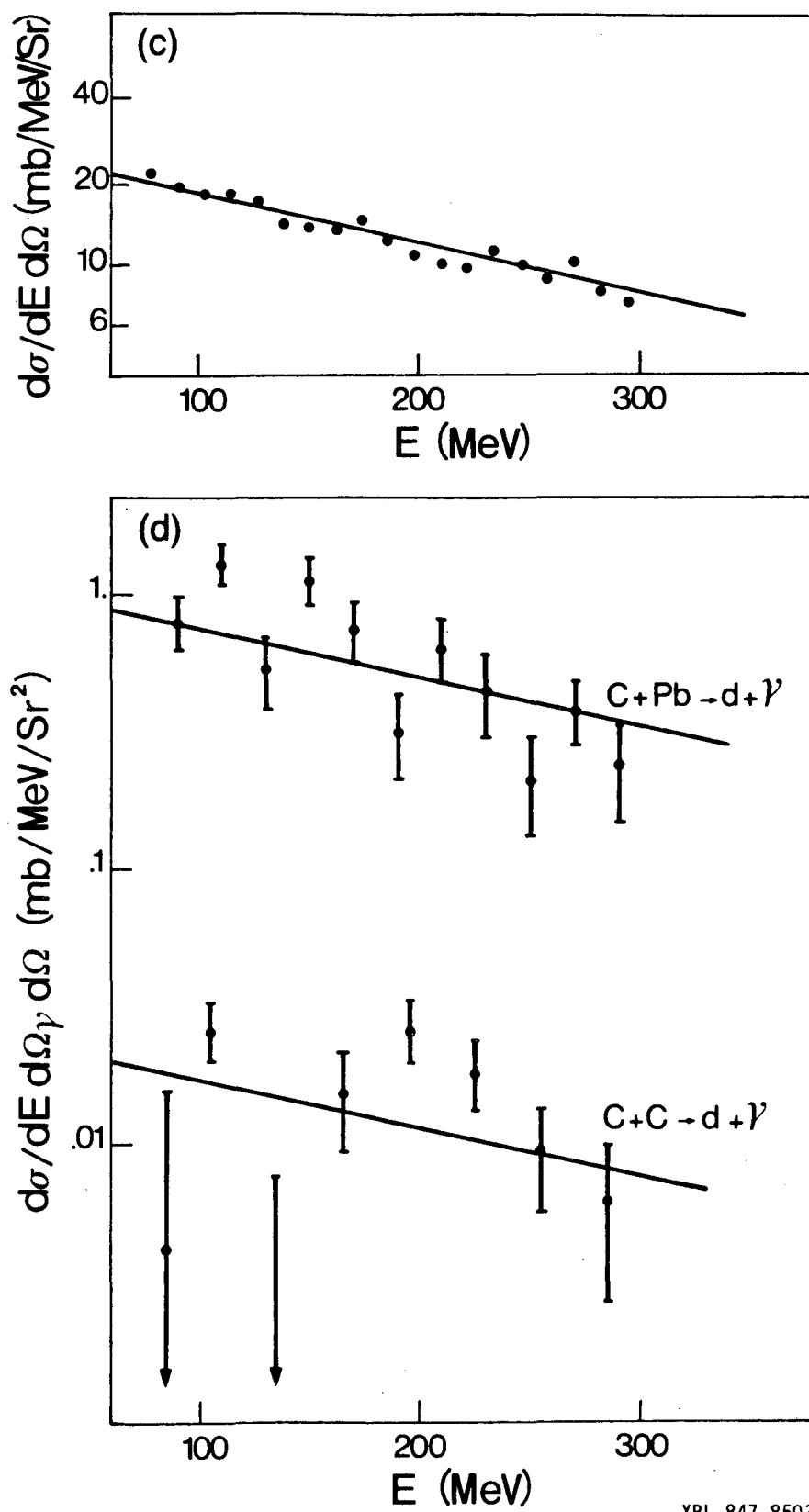
XBL 847-8505

Fig. 6d



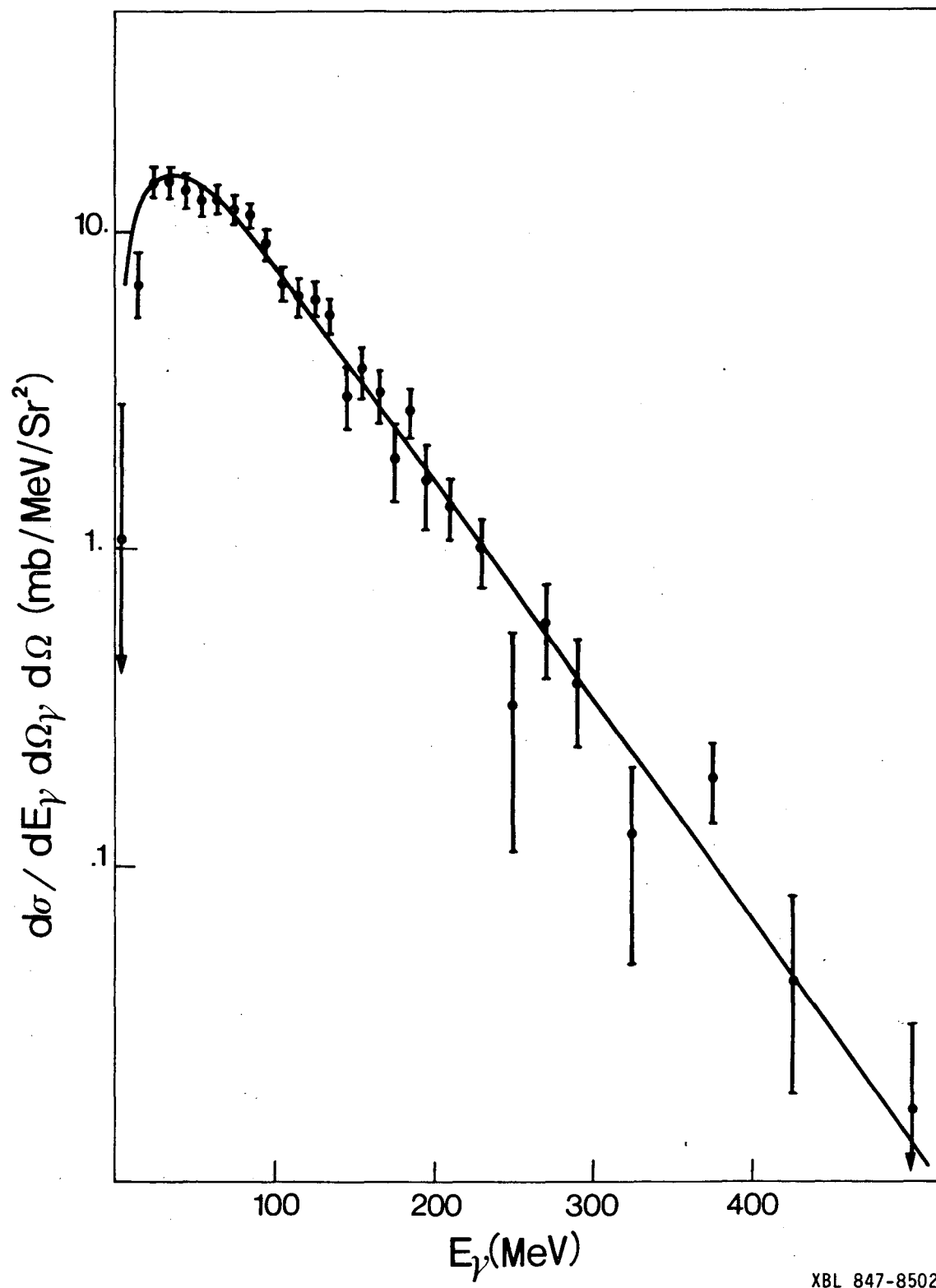
XBL 847-8504

Fig. 7a,b



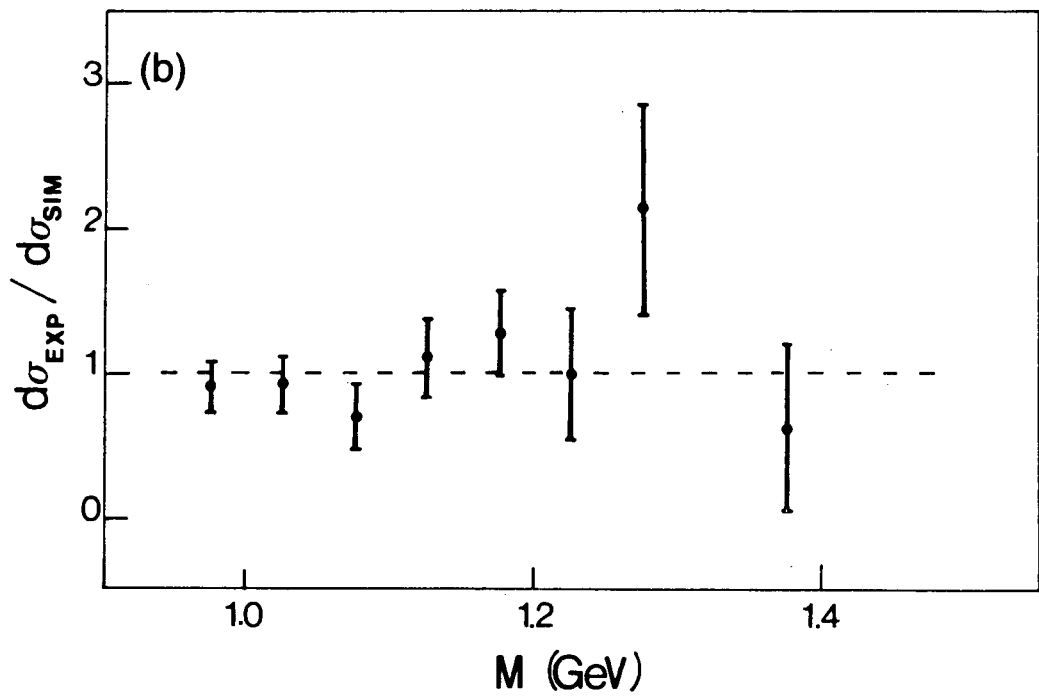
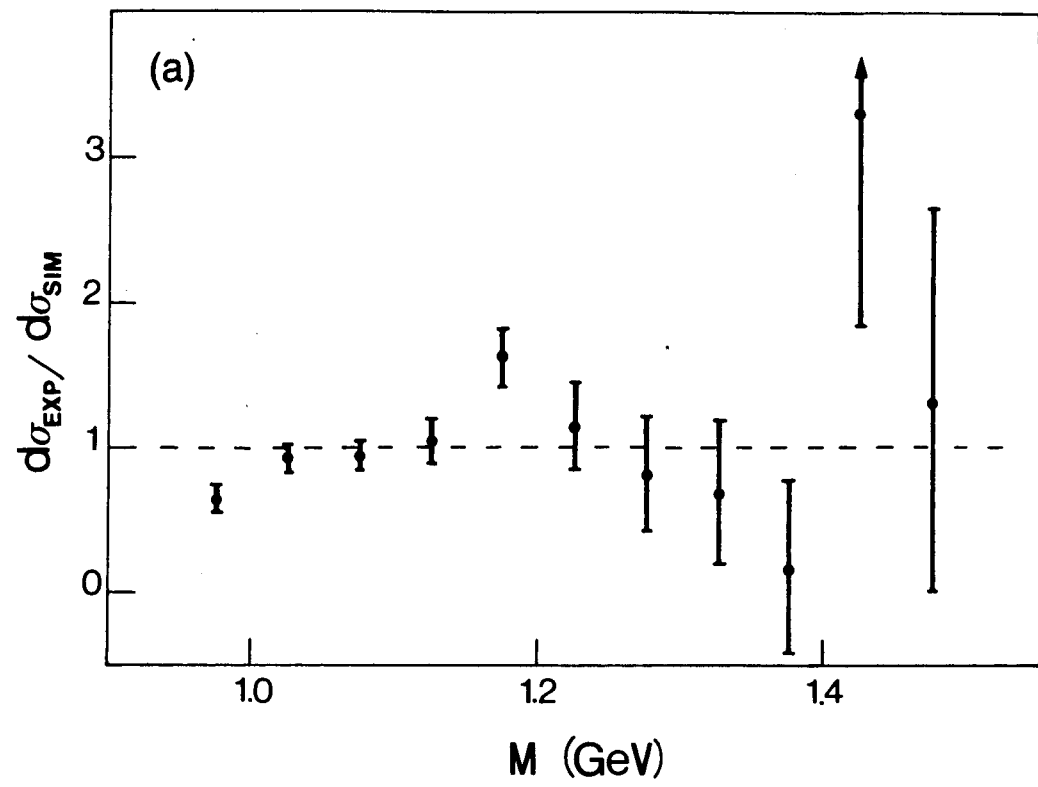
XBL 847-8503

Fig. 7c,d



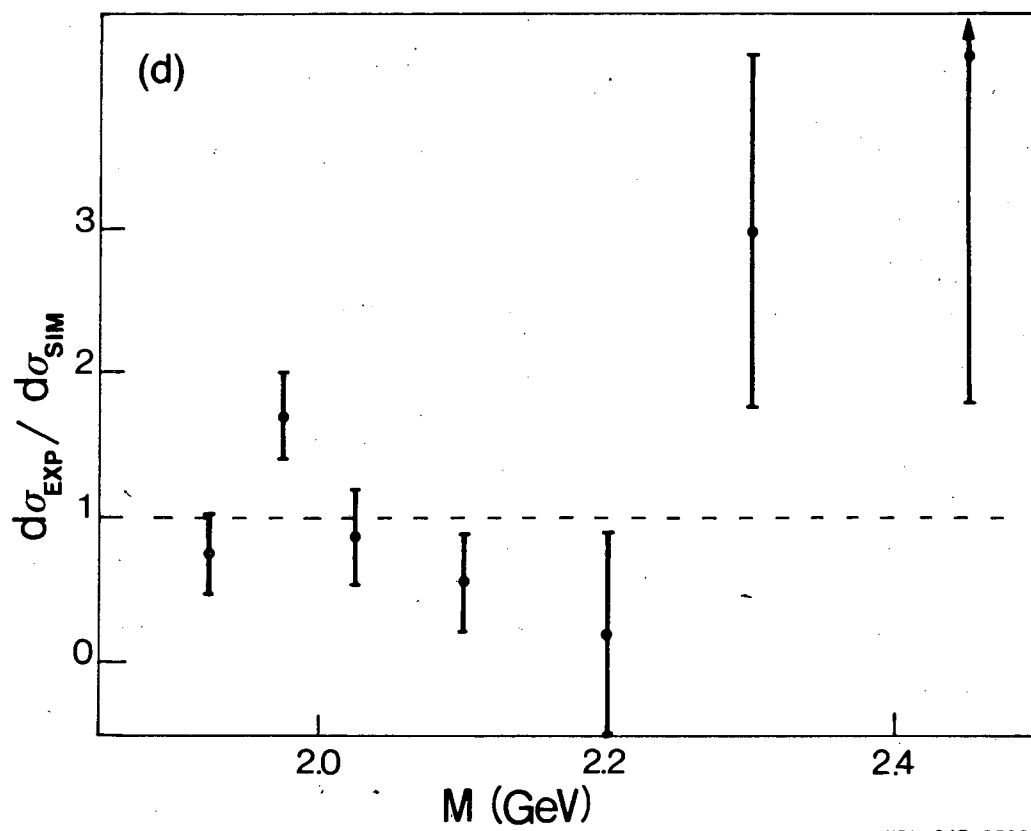
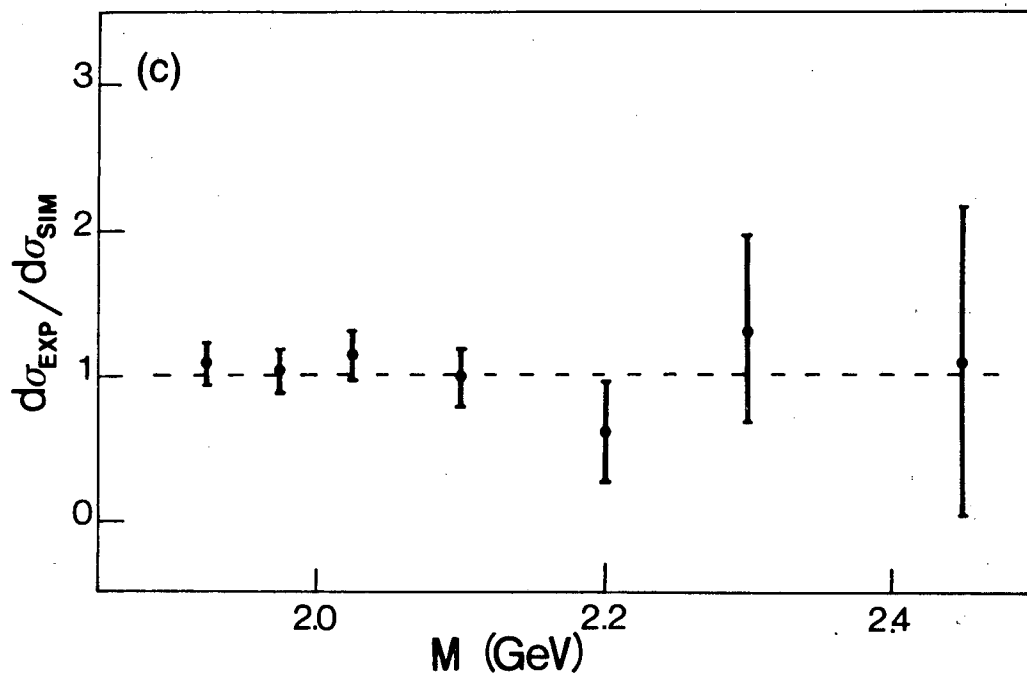
XBL 847-8502

Fig. 8



XBL 847-8501

Fig. 9a,b



XBL 847-8500

Fig. 9c,d

This report was done with support from the Department of Energy. Any conclusions or opinions expressed in this report represent solely those of the author(s) and not necessarily those of The Regents of the University of California, the Lawrence Berkeley Laboratory or the Department of Energy.

Reference to a company or product name does not imply approval or recommendation of the product by the University of California or the U.S. Department of Energy to the exclusion of others that may be suitable.

TECHNICAL INFORMATION DEPARTMENT
LAWRENCE BERKELEY LABORATORY
UNIVERSITY OF CALIFORNIA
BERKELEY, CALIFORNIA 94720